発表者氏名	論文タイトル名	発表誌名	巻号	ページ	出版年
Miura S Kawana K Schust DJ Fujii T Yokoyama T Iwasawa Y Nagamatsu T Adachi K Tomio A Tomio K Kojima S Yasugi T Kozuma S Taketani Y	CD1d, a sentinel molecule bridging innate and adaptive immunity, is downregulated by the human papillomavirus (HPV) E5 protein: a possible mechanism for immune evasion by HPV.	J Virol	84	11614-23	2010
Adachi K Kawana K Yokoyama T Fujii T Tomio A Miura S Tomio K Kojima S Oda K Sewaki T Yasugi T Kozuma S Taketani Y	Oral immunization with Lactobacillus casei vaccine expressing human papillomavirus (HPV) type 16 E7 is an effective strategy to induce mucosal cytotoxic lymphocyte against HPV16 E7.	Vaccine	28	2810-7	2010
Yamashita H Okuma K Kawana K Nakagawa S Oda K Yano T Kobayashi S Wakui R Ohtomo K Nakagawa K	Comparison Between Conventional Surgery Plus Postoperative Adjuvant Radiotherapy and Concurrent Chemoradiation for FIGO Stage IIB Cervical Carcinoma: A Retrospective Study.	Am J Clin Oncol,	Epub	Epub	2010
Okuma K Yamashita H Kawana K Nakagawa S Oda K Nakagawa K	Advanced age is a significant determinant of poor prognosis in patients treated with surgery plus postoperative radiotherapy for endometrial cancer.	J Obstet Gynecol Res	36	757-763	2010
Shoji K Oda K Nakagawa S Kawana K Yasugi T Ikeda Y Takazawa Y Kozuma S Taketani Y	Aromatase inhibitor anastrozole as a second-line hormonal treatment to a recurrent low-grade endometrial stromal sarcoma: a case report.	Med Oncol	Epub	Epub	2010

発表者氏名	論文タイトル名	発表誌名	巻号	ページ	出版年
Molvarec A., Shiozaki A., Ito M., Toldi G., Stenczer B., Szarka A., Nakashima A., Vásárhelyi B., Rigó J. Jr., Saito S.	Increased prevalence of peripheral blood granulysin-producing cytotoxic T lymphocytes in preeclampsia.	J Reprod Immunol			in press
Saito S, Nakashima A, Shima T,	Future directions of studies for recurrent miscarriage associated with immune etiologies.	J Reprod Immunol.			in press.
Yamashita K., Yoshioka Y., Higashisaka K., Mimura K., Morishita Y., Nozaki M., Yoshida T., Ogura T., Nabeshi H., Nagano K., Abe Y., Kamada H., Monobe Y., Imazawa T., Aoshima H., Shishido K., Kawai Y., Mayumi T., Tsunoda S., Itoh N., Yoshikawa T., Yanagihara I., Saito S., Tsutsumi Y.	Silica and titanium dioxide nanoparticles cause pregnancy complications in mice.	Nature Nanotechnology	6	321-328	2011
Molvarec A, Blois M S, Stenczer B, Toldi G, Tirado-Gonzalez I, Ito M, Shima T, Yoneda S, Vásárhelyi B, Rigó J., Saito S.	Peripheral blood galectin-1-expressing T and natural killer cells in normal pregnancy and preeclampsia.	Clin. Immunol	139	48-56	2011
Lin Y, Li C, Shan B, Wang W, Saito S, Xu J, Di J, Zhong Y, Li DJ.	Reduced stathmin-1 expression in NK cells associated with spontaneous abortion.	Am J Pathol.	178	506-514	2011

Nakashima A, Ito M, Yoneda S, Shiozaki A, Hidaka T, Saito S.	Circulating and decidual Th17 cell levels in healthy pregnancy.	*Am J Reprod. Immunol.*	63	104-109	2010
Nakashima A, Ito M, Shima T, Bac ND, Hidaka T, Saito S.	Accumulation of IL-17-positive cells in decidua of inevitable abortion cases.	Am J Reprod Immunol.	64	4-11	2010
Shima T., Sasaki Y., Itoh M., Nakashima A., Ishii N., Sugamura K., Saito S.	Regulatory T cells are necessary for implantation and maintenance during early stage of pregnancy, but not necessary during late stage of pregnancy in allogeneic mice.	J. Reprod Immunol,	85	121-129	2010
Saito S, Nakashima A, Shima T, Ito M.,	Th1/Th2/Th17 and regulatory T cell paradigm in pregnancy.	Am J Reprod Immunol.	63	601-610	2010
Saito S, Shima T, Nakashima A, Lin Y	Immune surveillance during pregnancy.	Ind. J. Physiol. Pharmacol.	54	60-63	2010
島　友子，中島彰俊，齋藤　滋	胎盤と免疫	周産期医学	40	1037-1042	2010
齋藤　滋，中島彰俊，島　友子	妊娠と免疫	周産期医学	40	1569-1573	2010

A Phagocytotic Inducer from Herbal Constituent, Pentagalloylglucose Enhances Lipoplex-Mediated Gene Transfection in Dendritic Cells

Shinichiro KATO,[a] Keiichi KOIZUMI,*[,a] Miyuki YAMADA,[a] Akiko INUJIMA,[a] Nobuhiro TAKENO,[a] Tsuyoshi NAKANISHI,[b] Hiroaki SAKURAI,[a] Shinsaku NAKAGAWA,[c] and Ikuo SAIKI[a]

[a] *Division of Pathogenic Biochemistry, Institute of Natural Medicine, University of Toyama; 2630 Sugitani, Toyama 930–0194, Japan;* [b] *Laboratory of Hygienics, Gifu Pharmaceutical University; 5–6–1 Mitahora-higashi, Gifu 502–8585, Japan; and* [c] *Department of Biotechnology and Therapeutics, Graduate School of Pharmaceutical Sciences, Osaka University; Suita, Osaka 565–0871, Japan.* Received May 6, 2010; accepted August 19, 2010

Antigen-presenting cells are key vehicles for delivering antigens in tumor immunotherapy, and the most potent of them are dendritic cells (DCs). Recent studies have demonstrated the usefulness of DCs genetically modified by lipofection in tumor immune therapy, although sufficient gene transduction into DCs is quite difficult. Here, we show that *Paeoniae radix*, herbal medicine, and the constituent, 1,2,3,4,6-penta-*O*-galloyl-β-D-glucose (PGG), have an attractive function to enhance phagocytosis in murine dendritic cell lines, DC2.4 cells. In particular, PGG in combination with lipofectin (LPF) enhanced phagocytic activity. Furthermore, PGG enhanced lipofection efficacy in DC2.4 cells, but not in colorectal carcinoma cell lines, Colon26. In other words, PGG synergistically enhanced the effect of lipofectin-dependent phagocytosis on phagocytic cells. Hence, according to our data, PGG could be an effective aid in lipofection using dendritic cells. Furthermore, these findings provide an expectation that constituents from herbal plant enhance lipofection efficacy.

Key words dendritic cell; lipofection; 1,2,3,4,6-penta-*O*-galloyl-β-D-glucose; phagocytosis

Dendritic cells (DCs) play a pivotal role in initiating and controlling the T cell-dependent immune response.[1] Immature DCs, localized in non-lymphoid tissues, have optimal capabilities for antigen uptake, processing and the formation of peptide-major histocompatibility (MHC) complexes. Antigen uptake and some cytokines, for example, in the inflammatory environment, promote their maturation and migration to T cell areas of regional lymphoid tissues, where matured DCs strongly present MHC class I and II restricted peptides to naïve T cells, inducing an immune response and differentiation.[2,3] Because of these properties, DCs have been considered quite attractive immune cells to achieve gene transduction for DNA-based immunization in tumor immunotherapy[4—7] and many gene delivery methods have attempted to optimize transduction and transfection to human and murine dendritic cells.[8—10]

However, despite advances in the understanding of DC biology, the development of genetic immunization strategies using DC-transfected plasmid DNA has been limited by their low transfection efficiencies.[11] Currently, the most efficient method for DC transduction is infection using a viral vector based on poxvirus, lentivirus, and adenovirus,[8,12,13] but viral vectors may be associated with safety concerns and generally require DNA codon optimization to overcome poor gene expression.[14,15] An attractive alternative to vector-mediated delivery into DCs is lipofection, non-viral gene transduction. The main advantages of lipofection are its ability to transfect all types of nucleic acids in a wide range of cell types, its ease of use, reproducibility and low toxicity.[16] Furthermore, recent studies have demonstrated the usefulness of DCs genetically modified by lipofection in tumor immunotherapy,[17] while sufficient gene transduction to DCs is quite difficult.[18] Therefore, it is easily thought that more efficient (DNA-based) DC vaccine therapy could be developed by not only understanding DC immune biology but also finding methods or substances which enhance lipofection efficiency in DCs.

We have sought out immunomodulating compounds derived from herbal medicine or Kampo preparations (formulation) for cancer therapy, especially metastasis.[19,20] In this study, we found that 1,2,3,4,6-penta-*O*-galloyl-β-D-glucose (PGG), which is contained in *Paeoniae radix* (roots of Paeonie lactiflora),[21] enhanced phagocytosis in murine a denndritic cell line, DC2.4, especially in combination with lipofectin (LPF). Lipofectin reagent (LPF; Invitrogen, CA, U.S.A.) is a cationic liposome, mixture of *N*-[1-(2,3-dioleyloxy)propyl]-*n*,*n*,*n*-trimethylammonium chloride (DOTMA) and dioleoyl phosphotidylethanol amine (DOPE) at 1 : 1 (w/w), and is widely used as a device for transfection of RNA, DNA, oligonucleotide and protein.[22—26]

These results motivated us to explore the effect of PGG on DC2.4 cells. PGG is a naturally occurring polyphenolic compound contained in many medical plants[27,28] and a number of studies have reported that PGG exhibits diverse bioactivity, for example, anti-tumor, anti-oxidant, and anti-inflammatory effects.[29] However, the effect of PGG on the phagocytosis of dendritic cells (DCs) has not been investigated, while th effect of polyphenol and tannins (a polyphenol) on phagocytosis and dendritic cells have been investigated well.[30—32] Phagocytosed exogenous antigens complexed with LPF induce high-antigen presentation *via* MHC class I and II and cytotoxic T lymphocytes (CTLs).[33,34] Hence, PGG may be a powerful candidate for tumor immunetherapy because it enhances the phagocytic effect of DC2.4 cells.

On the other hand, we hypothesized that PGG could enhance lipofection efficacy and have a new application for lipofection on DCs because lipofection largely depends on the phagocytic effect,[35] therefore, the present study investigated the effect of PGG on lipofection efficacy in DC2.4 and bone marrow-derived dendritic cells (BMDCs). Moreover, to demonstrate whether the effect of PGG depends on phagocytosis, we also tested the effect on Colon 26, murine colorectal carcinoma cell line. According to our data, the enhancement of lipofection efficacy by PGG was specific for dendritic cells and PGG could be a seed compound of an effective aid

* To whom correspondence should be addressed. e-mail: kkoizumi@inm.u-toyama ac.jp

for lipofection.

MATERIALS AND METHODS

Reagents AIM-V and Opti-MEM were purchased from Invitrogen (Carlsbad, CA, U.S.A.)/ GIBCO BRL (Grand Island, New York, U.S.A.). The aqueous extraction from *Paeoniae radix* was performed, as previously mentioned.[36] Briefly, about 45 g dried and cut roots were brewed with 900 ml water. Then the filtrate was collected after filtration. The residue was boiled with 800 ml water again and added in the filtrate after filtration. The filtrate was lysophilized. The powder was stored at 4 °C. The concentration used in the experiment was based on the dry weight of the extract (mg/ml). 1,2,3,4,6-penta-*O*-galloyl-*β*-D-glucose (PGG) was purchased from Toronto Research Chemicals Inc. PGG stock solution, originally dissolved to a concentration of 5 mM in 100% dimethyl sulfoxide (DMSO). Paeoniflorin was purchased from Wako Pure Chemical Industries, Ltd. (Osaka, Japan) Paeoniflorin and Gallic acid (GA) stock solution originally dissolved to a concentration of 10 mM in distillated water. 1,3,6-tri-*O*-galloyl-*β*-D-glucose (TGG) stock solution originally dissolved to a concentration of 10 mM in 100% DMSO. These all chemical compounds were diluted to the desired concentration in AIM-V or Opti-MEM just before using.

Cell Culture DC2.4 cell, derived from a c57BL/6 immature dendritic cell line, was maintained in RPMI1640 supplemented with 50 μM β-melcaptoethanol. Colon26, derived from BALB/c colorectal cancer, was maintained with RPMI1640 supplemented with 2 mM L-glutamine. All media contained 10% fetal calf serum (FCS), 100 U/ml penicillin and 100 mg/ml streptomycin, and cultures were kept at 37 °C in a humidified atmosphere of 5% CO_2/95% air.

Phagocysosis in DC2.4 Fluorescence isothiocianate (FITC) conjugated-dextran (average molecular weight 40 kDa) was purchased from SIGMA-ALDRICH (St. Louis, MO, U.S.A.) and originally dissolved to a concentration of 10 mg/ml in balanced salt solution (BSS). Phagocytosis in DC2.4 was performed by modification of a previously reported method.[37] In this assay, AIM-V media was used instead of growth media. Briefly, 1×10^5 cells/well were seeded in a 24-well plate (Corning corter) and pre-incubated with PGG for 1.5 h at 37 °C. Pre-treated DC2.4 was phagocytosed in the presence of 10—500 μg/ml FITC-dextran or lipoplex for 1 h at 37 °C, which was made of FITC-dextran and 20 μl Lipofectin (Invitrogen) by co-incubation for 35 min. To inhibit phagocytosis of DC2.4 cells, DC2.4 cells were pre-incubated with wortmannin (final concentration; 5 μM) for 20 min before addition of FITC-dextran. FITC-positive cells were detected by fluorescence microscopy using a Keyence fluorescence microscope. For quantitative determinations of transfection efficiency, fluorescent cells were assessed by fluorescence-activated cell sorting (FACS) using a FACSCalibur flow cytometer (Becton-Dickinson, Mountain View, CA, U.S.A.) and CellQuest software.

Differentiation of Bone Marrow-Derived Dendritic Cells Bone marrow-derived dendritic cells (BMDCs) were differentiated from c57BL/6NCrSlc (9—10-weeks-old specific pathogen free female, Japan SLC (Hamamatsu, Japan)) as reported previously.[38] Differentiated BMDCs were qualified by immunophenotypes and phagocytic activity using FITC-dextran and we used defined BMDCs which express both CD11c and MHC class II more than 70% of total population.

Plasmids The vectors encoding green fluorescent protein (GFP) mutant, pEGFP-N1 and pEGFP-C1, were purchased from Clontech (Palo Alto, CA, U.S.A.). These vectors encode a mutant GFP that contains more than 190 silent nucleotide changes to optimize the coding sequence based on human codon-usage preferences,[39] and mutations at residue 64 (Phe→Leu) and 65 (Ser→Thr), which results in enhanced fluorescence and a single excitation peak at 488 nm.

Lipofection and Transgenes Expression Lipofection using a lipofectin reagent was performed by following the modified instructions of the manufacture. One day before transfection, 2×10^5 cells were seeded in growth media, and nearly 60% confluent cells were used for lipofection. Four microliters of lipofectin reagent was diluted in 100 μl Opti-MEM in one tube and incubated for 30 min at room temperature. Meanwhile, 2—4 μl pEGFP-N1 (1 μg/μl) and pEGFP-C1 (1 μg/μl) (Clontech) were diluted in 100 μl Opti-MEM in another tube separately for 15 min at room temperature. The transfection reagents and plasmid solution were then mixed and incubated at room temperature based on the manufacturer's instructions. Cells were familiarized with Opti-MEM for 30 min before lipofection. Eight-hundred microliters of Opti-MEM were added to the mixed solution (finally 200 μl+800 μl), then after removal of the conditioned Opti-MEM, cells were added to transfection solutions (1 ml) and incubated for 5 h. After lipofection for 5 h, transfection solution was replaced with growth media. In PGG-assisted lipofection, PGG was used for incubation of lipoplex throughout lipofection. Twenty-four hours following lipofection, enhanced green fluorescent protein (EGFP)-positive cells were detected and quantified by the same methods as for the phagocytosis of DC2.4.

Flow Cytometric Analysis and Immunophenotypic Analysis After removal of the supernatant, cells were split off using 0.13% trypsin and ethylenediaminetetraacetic acid (EDTA), pelleted by centrifugation, resuspended in phosphate buffered saline (PBS) containing 2% FCS to a final density of $\sim5\times10^6$ cells/ml, and filtered through a nylon membrane to remove cell aggregates. Flow cytometry for EGFP and propidium iodide (PI) fluorescence were performed using a FACSCalibur (BD Bioscience). For immunophenotypic analysis of DC2.4 cells, split cells were suspended in FACS buffer ($0.5—1\times10^6$ cells/50 μl), containing PBS in 0.02% NaN_3 (w/v) and 2% FCS (v/v). Cells were first incubated with an antibody against FcRg (clone 2.4G2) for 5 min and then labeled with antibodies against CD80 (clone 16-10A1), CD86 (clone GL1), MHC class I (clone 28-14-8) and MHC class II (clone M5/114.15.2) for 30 min. All polyethylene (PE)-conjugated mAb were acquired from BD Biosciences.

Statistical Analysis Three means (±1 S.D.) were composed using analysis of variance (ANOVA) (Figs. 1, 3). Two means (±1 S.D.) were composed using the unpaired Student's *t*-test (two tailed) (Figs. 2, 4). A p value of less than 0.05 was considered significant.

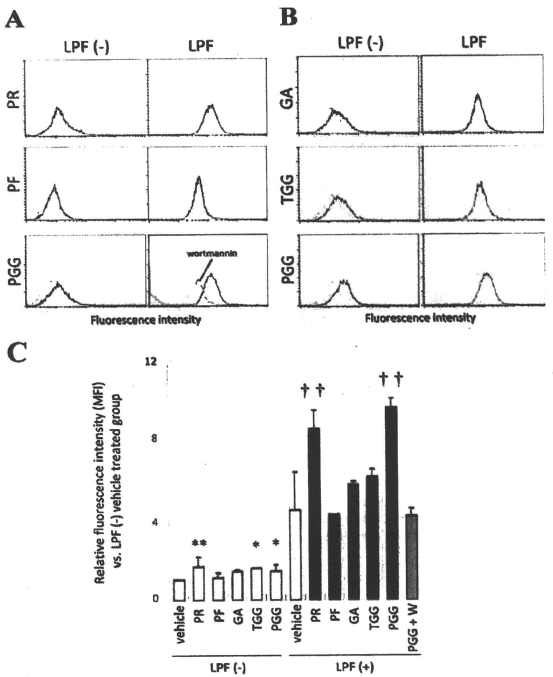

Fig. 1. Ability of 1,2,3,4,6-Penta-*O*-galloyl-β-D-glucose (PGG) to Phagocytose into DC2.4

After pre-incubation with (A) 1 mg/ml *Paeoniae radix* (PR), 10 mM Paeoniflorin (PF) or 10 mM PGG and (B) 10 mM gallic acid (GA), 10 mM 1,3,6-tri-*O*-galloyl-β-D-glucose (TGG) or 10 mM PGG for 1.5 h, DC2.4 phagocytosed for 1 h at 37 °C in the presense of 250 mg/ml FITC-dextran combined without (left) or with (right) Lipofectin (LPF). Phagocytosed DC2.4 were analyzed by flow cytometer. Filled profile, non-treated cells as control; gray dotted line, FITC-dextran without preincubation with indicated compounds; black line, FITC-dextran with preincubation with indicated compounds, FITC-dextran with preincubation with PGG and 5 μM wortmannin (abbreviation: W) to inhibit phagocytosis. Data are representative of at least two independent experiments. (C) Relative mean fluorescence intensity (MFI) as phagocytic activity was assessed by flow cytometry. Data are presented as the means±S.D. of at least two independent experiments. * $p<0.05$, ** $p<0.01$, *vs.* LPF (−) vehicle group, †† $p<0.01$, *vs.* LPF (+) vehicle group by analysis of variance (ANOVA) with Bonferroni correction.

RESULTS AND DISCUSSION

Phagocytosis in DC2.4 Cells Was Enhanced by 1,2,3,4,6-Penta-*O*-galloyl-β-D-glucose (PGG) Recently, we found that the ability of *Paeonie radix* (aqueous extractions) to engulf FITC-dextran into DC2.4 cells occurred in an FITC-dextran and *Paeonie radix* (PR) (Figs. 1A, C). To identify which chemical compounds enhanced engulfment in DC2.4 cells from *Paeonie radix*, we tested the effect of paeoniflorin (PF) and PGG, contained in PR,[27] on incorporation of FITC-dextran in DC2.4 cells. Of these compounds, PGG enhanced engulfment in DC2.4 cells at the same level as PR, while PF, which is the major compound contained in PR, hardly enhanced engulfment (Fig. 1A). PGG had little effect on engulfment with FITC-dextran alone but engulfment was apparently enhanced with the FITC-dextran/lipofectin (LPF) complex (Fig. 1C). The effect was cancelled by wortmannin, a phagocytosis inhibitor,[40] suggesting that the increase of intracellular FITC-dextran depended on the enhancement of phagocytic activity (Figs. 1A, C). This means that PGG synergistically enhances phagocytosis in combination with LPF in DC2.4 cells. In this property, PGG is utilized for lipofection using LPF. Furthermore, we also found the importance of the chemical structure of PGG in the enhancement of phagocytosis in DC2.4 cells (Figs. 1B, C). PGG has five ester bonds formed between the hydroxyl group of the glucose backbone and the carboxyl group of gallic acid (GA).[29] 1,3,6-Tri-*O*-galloyl-β-D-glucose (TGG), which has three ester bonds, enhanced the phagocytosis of DC2.4 in the absence of LPF and had a tendency to enhance

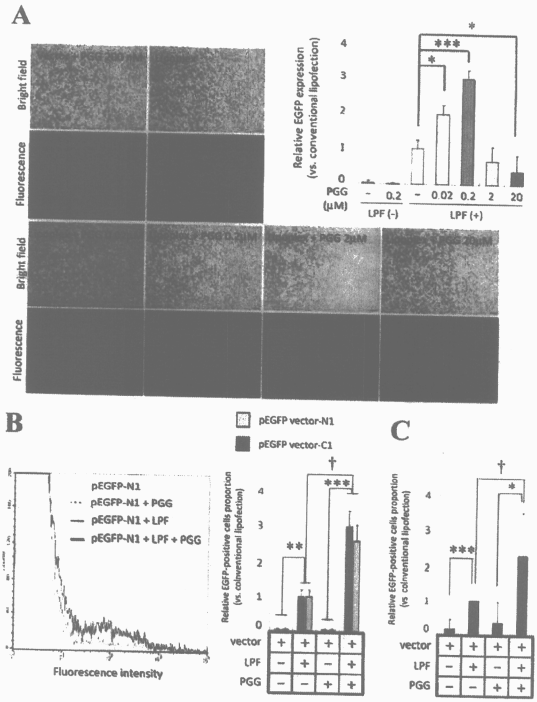

Fig. 2. Lipofection with Lipofectin (LPF) Combined with PGG in DC2.4 and Bone Marrow Derived Dendritic Cells

DC2.4 bone marrow derived dendritic cells were transfected with LPF and PGG together for 5 h. After 24 h of culture with growth medium at 37 °C, EGFP expression was obtained by fluorescence microscopy and flow cytometry. (A) Transfected DC2.4 cells with 2 μg pEGFP-N1 vector with 200 nM PGG (without Lipofection) (upper left), vector+LPF (lipoplex) (upper right), vector+LPF+PGG indicated concentration (lower panel). Up and downward square observe pictures under phase-contact microscopy and fluorescence image. Scale bar=100 μm. EGFP gene transduction of DC2.4 lipofected with indicated PGG concentration was expressed as EGFP expression (relative EGFP-positive cell proportion (fold)). (B) Histogram image shows EGFP intensity on DC2.4 cells transfected respectively. EGFP gene transduction of DC2.4 lipofected with indicated combination was expressed as EGFP expression (relative EGFP-positive cell proportion (fold)). (C) EGFP gene transduction of BMDCs lipofected with 4 μg pEGFP vector and indicated combination was expressed as EGFP expression (relative EGFP-positive cell proportion *vs.* conventional lipofection (fold)). Data are presented as the means±S.D. of (B) five or (C) three independent experiments. $*p<0.05$, $**p<0.01$, $***p<0.005$, *vs.* respective LPF-untreated group. $\dagger p<0.01$, *vs.* PGG-untreated group by two-tail unpaired Student's *t*-test.

phagocytosis in the presence of LPF but the enhancement was lower than that of PGG. Additionally, GA also had a tendency to enhance phagocytosis, and the enhancement of GA was lower than that of TGG, suggesting that the ester binding mode between the glucose core and gallic acid rather than gallic acid itself is strongly involved in the enhancement of phagocytosis in DC2.4 cells (Fig. 1B).

Enhanced the Efficacy of Lipofection Using PGG in Mouse Dendritic Cells Gene transfer into DCs is critical for potential therapeutic applications as well as for study of the genetic basis of DC-mediated immunological development and immune regulation, however, transfection into DCs is difficult.[11] In particular, it is difficult to transduce naked or plasmid DNA on DCs.[9] The main advantages of lipofection are its ability to transfect all types of nucleic acids in a wide range of cell types, its ease of use, reproducibility and low toxicity,[16] therefore, development of more efficient lipofection must enable DC vaccine therapy, and knowledge of DCs biology should be disseminated.

Thus, we tested the effect of PGG on lipofection in DC2.4 cells because PGG enhanced phagocytic activity. In pilot studies of our lipofection, we determined the optimal concentrations of the transfection reagent, plasmid vector and the length of incubation required for the best expression of EGFP in DC2.4 cells. We basically performed lipofection according to the instructions of the manufactures using a GFP

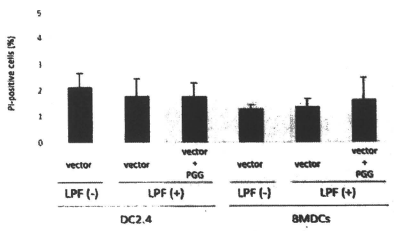

Fig. 3. Effect for Combination of Lipofectin (LPF) and 1,2,3,4,6-Penta-*O*-galloyl-β-D-glucose (PGG) in DC2.4 and BMDCs for Cell Viability

After 24 h of transfection, Propium iodide (PI) staining as DC2.4 and BMDCs viability was determined by flow cytometry. Data are presented as the means±S.D. of three independent experiments. No significant difference by ANOVA.

reporter construct, pEGFP-N1 and pEGFP-C1 vector to determine lipofection efficacy at 24 h posttransfection. For lipofection, we used 2 μg pEGFP-N1 or pEGFP-C1 vector as cytotoxicity (*i.e.*, cell detachment) was noted at higher amounts (data not shown) and 4 μl LPF. Lipofectin required an incubation period of >1 h with DC2.4 cells, whereas optimal results were obtained with about 5-h incubation in serum-free medium (EGFP-positive ($EGFP^+$) cells; 2.7±0.9%, n=5). Our lipofection efficacy corresponds to previous studies using lipofection in dendritic cells (lipofection efficacy is less than 2% or not detectable.).[9,41]

To evalutate the effect of PGG on lipofection, we used PGG in the preceding lipofection during incubation to prepare the pEGFP vector/LPF complex (lipoplex) for lipofection, and determined the efficacy of EGFP for lipofection efficacy by flow cytometry and fluorescent microscopy. PGG expectedly enhanced the expression of EGFP (Fig. 2) and enhancement was achived in a concentration-dependent manner, but more than 2 μM PGG did not enhance the expression of EGFP (Fig. 2A). Furthermore, DC2.4 cells transfected with pEGFP-N1 vector in combination with 200 nM PGG (without LPF) produced no detectable EGFP fluorescence. A similar phenomenon was also obtained for phagocytic activity in DC2.4 (Fig. 1). Hence, PGG synergistically enhanced phagocytosis and lipofection using LPF. A similar result was obtained using another vector, pEGFP-C1 (Fig. 2B). Thus, transfection activity in an immature dendritic cell line DC2.4 cells was highly enhanced by PGG.

To sophisticate and assess the function of PGG as an inducer of lipofection, we used bone marrow derived dendritic cells (BMDCs) instead of DC2.4 cells. BMDCs were evaluated by flowcytometer and phagocytic activity using FITC-dextran. BMDCs express both CD11c and MHC class II more than 70% of total population were used in our experiments and lipofection procedure on DC2.4 was also applied to BMDCs except for amount of plasmid vector, 2 μg plasmid vector changed to 4 μg. As a result, although the effect of PGG on lipofection efficacy in BMDCs did not seem to be strong, it was significantly enhanced (Fig. 2C). Therefore, PGG could enhance the lipofection efficacy in dendritic cell- or phagocytic cell-specific manner.

Effect of Lipofection with PGG on Dendritic Cells Viability In addition to measuring EGFP expression at 24 h posttransfection, we assessed the effect of lipofection combined with PGG on cell viability by staining with propium iodide (PI) and using a flow cytometer. In Fig. 3, DC2.4 and BMDCs were not damaged by lipofectin in combination with PGG, and 200 nM PGG by itself also did not exhibit cytotoxicity on these cells (determined using WST-1: cell proliferation assay; data not shown). PGG might not exhibit remarkable cytotoxicity because of the low concentration. Usually, non-viral transfections are harmful to DCs[9,17] and lipoplex can increase cytotoxicity along with lipofection efficacy in a dose-dependent manner.[42] Clinically, all vaccines and DNA-based DC vaccine therapies must be safe, therefore, PGG would be a useful aid for lipofection.

Does Lipofection in Combination with PGG Depend on Phagocytosis? We have suggested that PGG enhanced the effect of lipofection on DC2.4 cells and BMDCs, however, the action mechanism of PGG is still unclear. Although one possibility was shown that PGG enhanced phagocytic activity in DC2.4 cells (Fig. 1), it remained to be confirmed. PGG may also enhance lipofection efficacy by increasing phagocytic activity. In the next study, to determine whether the effect of PGG on lipofection depends on phagocytosis, we tested its effect using colon 26 cells, a murine colon carcinoma cell line. The endocytocytic lipoplex uptake pathway is further separated into phagocytosis (phagocytic cells) and pinocytosis (all cells).[43] As shown in Fig. 4, PGG slightly enhanced lipofection efficacy on colon 26 but not significantly, therefore, the enhancement of lipofection efficacy on DC2.4 and BMDCs by PGG greatly depend on intensified phagocytosis and is not implicated in the fusogenic effect. Namely, the effect of PGG would be restricted to phagocytic cells, like DCs.

The internalization mechanism of lipoplex is not well understood. An early report suggested that the fusogenic effect between the positively charged lipoplex and the plasma membrane is responsible for tranducing DNA into cytosol,[22] however, subsequent studies recently have shown the involvement of phagocytosis in delivering DNA.[44,45] Hence, it is currently believed along with this historical background that membrane fusion is important in lipofection but uptake of lipoplex largely depends on phagocytosis and endocytosis. According to our data, PGG specifically enhanced lipofection efficacy in DC2.4 cells and BMDCs. In other words, PGG enhanced some functions specifically found in DCs. Additionally, it was thought that phagocytosis facilitated by PGG enhanced lipofection efficacy.

A remaining question for our further study is which site of action of PGG is responsible for phagocytosis. In our lipofection protocol, PGG was added during the generation of lipoplex and transfection; namely, PGG affects lipoplex, DC2.4 or both to enhance lipofection efficacy.

If PGG modified lipoplex more effectively by making a lipoplex/PGG complex, PGG must enhance lipofection efficacy on colon 26 cells. It is unknown why they make a complex with each other, but the lipoplex/PGG complex must be phagocytosed through a DC-specific receptor. The recent identification of surface receptors expressed on DCs allow for a specific target for effective transfection.[46] Receptors such as $Fc\gamma RI$[47,48] and mannose[49,50] are attractive candidates for target cell surface molecules. If PGG has an affinity with

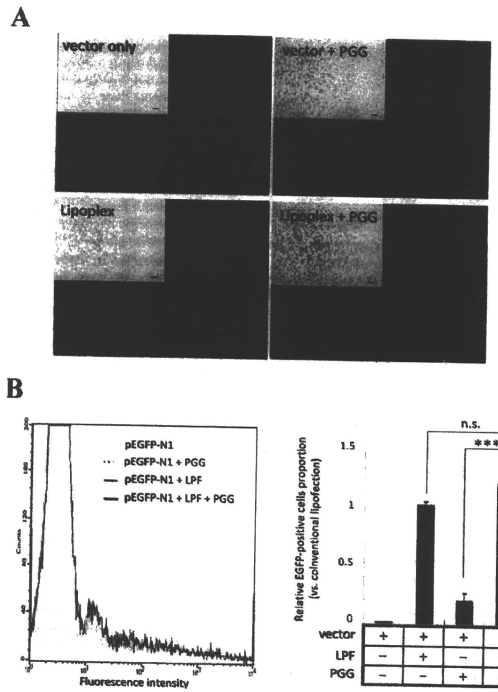

Fig. 4. Lipofection with Lipofectin (LPF) Combined with PGG in Colon 26

Colon 26 cells were transfected with LPF and PGG together. Lipofection and detection of EGFP used the same methods as for DC2.4 cells (*cf.* Fig. 2). (A) Transfected colon 26 with 2 μg pEGFP-N1 vector only (without Lipofection) (upper left), vector+200 nM PGG (upper right), vector+LPF (lower left), vector+LPF+200 nM PGG (lower right). Small squares show images under phase-contact microscopy. Scale bar=100 μm. (B) EGFP gene transduction of colon 26 lipofected with the indicated combination was expressed as EGFP expression (EGFP-positive cell proportion (%)). Data are presented as the means±S.D. of two or three independent experiments. $***p<0.005$, *vs* respective LPF-untreated group by two-tail unpaired Student's *t*-test. n.s.=no significant difference.

these cell surface receptors, the lipoplex/PGG complex may be easily phagocytosed. In previous studies, Li *et al.* reported that PGG binds to cell surface insulin receptor[51] and a number of researchers have studied the binding activity to biomolecules of PGG[29]; however it remains to be determined whether PGG binds to a DC-specific cell surface receptor. Furthermore, we have already suggested the importance of lipoplex incubation in combination with PGG for effective lipofection (data not shown). Consequently, we need to investigate the binding activity to cell surface receptor on DC2.4 cells and BMDCs in our further studies.

Secondly, we should focus on the DC maturation state if the action mechanism depends on the enhancement of phagocytosis. DCs have high phagocytic properties in the immature state, while few phagocytic properties in the mature state. Although DCs can phagocytose, they can be transformed by lipofection only with very low efficacy, perhaps due to their high nuclease content or easy of maturity by transfection. In this study, we used an immortalized murine immature DC line, DC2.4 cells[21] and primary immature BMDCs. These cells may be maturated by lipofection and lose phagocytic activity. As one possibility, PGG could maintain the phagocytic activity by inhibiting their maturation. DC maturation and differentiation are regulated by nuclear factor κB 2 (NF-κB2) and RelB, and these proteins are involved in vesicular transport.[52—54] Because previous reports have shown the inhibitory effect of PGG on NF-κB activity,[29,55] PGG probably maintaines an immature state by inhibiting a transcriptional factor, such as NF-κB. However, it has been reported that lipofectin alone or lipoplex could not induce maturation on DCs related to the cell surface expression of major histocompatibility (MHC) class I or II, CD40,

CD80, CD86, ICAM-I and IL-12 p40 expression,[33,34,53] and an inflammatory signal, LPS, was needed to change immature DCs into mature DCs.[56] Our phenotypical analysis of DC2.4 cells correspondingly demonstrated that cell surface expressions of MHC class II and CD80 were hardly increased by lipofection but were not inhibited by PGG (data not shown). Thus, we considered that PGG did not suppress DC maturation to maintain phagocytic activity.

Our data showed that PGG affected phagocytosis and lipofection efficacy in DC2.4 cells but the action mechanism has not been clarified. Hereafter, we must elucidate the mechanism in detail to understand DC biology and structure for a more highly effective lipofection method. If these challenges are achieved, DC vaccine therapy will develop markedly. Conventional DC vaccine therapies have already succeeded to some extent. In addition to these conventional therapies, DC vaccine therapy is expected to be highly effective and to be refined by more efficient lipofection of cytokines,[57] chemokines[58] and tumor-associated antigens (TAAs) using PGG.

Herbal medicine and medicinal plants have been used against a lot of diseases all over the world and considered enormous chemical library. Actually, various compounds have been found in medicinal plants, for example; resveratrol in grapes and the red wine prepared from them.[32] But, these reports showed only biological activities of medicinal plant-derived compounds. Our studies exhibit not only biological activities but also the pharmaceutical technological effectiveness as an application. Finally, our present findings provide an expectation that constituents from herbal plant enhance lipofection efficacy.

Acknowledgements This study was supported by a Grant for Health and Labour Sciences Research (H22-RINSHO KENKYU SUISHIN KENKYU-013 and SOUYAKU SOGO SUISHIN KENKYU-007) from the Ministry of Health Labour and Welfare, Japan. We thank Dr. N. Kageyama (Yahara) and Dr. M. Kadowaki, Division of Gastrointestinal Pathophysiology, Department of Bioscience, Institute of Natural Medicine, University of Toyama, for helpful advices and technical supports and Dr. N. Okada, Department of Biotechnology and Therapeutics, Graduate School of Pharmaceutical Sciences, Osaka University, for technical information and procedure about differentiation of BMDCs.

REFERENCES

1) Itano A. A., Jenkins M. K., *Nat. Immunol.*, **4**, 733—739 (2003).
2) Austyn J. M., *J. Exp. Med.*, **183**, 1287—1292 (1996).
3) Muriel M., Kenneth M. M., *Nat. Immunol.*, **1**, 199—205 (2000).
4) Falo L. D. Jr., Kovacsovics-Bankowski M., Thompson K., Rock K. L., *Nat. Med.*, **1**, 649—653 (1995).
5) Banchereau J., Palucka A. K., *Nat. Rev. Immunol.*, **5**, 296—306 (2005).
6) Gilboa E., *J. Clin. Invest.*, **117**, 1195—1203 (2007).
7) Nestle F. O., Farkas A., Conrad C., *Curr. Opin. Immunol.*, **17**, 163—169 (2005).
8) Okada N., Tsukada Y., Nakagawa S., Mizuguchi H., Mori K., Saito T., Fujita T., Yamamoto A., Hayakawa T., Mayumi T., *Biochem. Biophys. Res. Commun.*, **282**, 173—179 (2001).
9) Melhem N. M., Gleason S. M., Liu X. D., Barratt-Boyes S. M., *Clin. Vaccine Immunol.*, **15**, 1337—1344 (2008).
10) Larregina A. T., Morelli A. E., Tkacheva O., Erdos G., Donalnue C., Watkins S. C., Thomson A. W., Falo L. D. Jr., *Blood*, **103**, 811—819 (2004).
11) Irvine A. S., Trinder P. K., Laughton, D. L., Ketteringham H., McDermott R. H., Reid S. C., Haines A. M., Amir A., Husain R., Doshi R., Young L. S., Mountain A., *Nat. Biotechnol.*, **18**, 1273—1278 (2001).
12) Flatz L., Hegazy A. N., Bergthaler A., Verschoor A., Claus C., Fernandez M., Gattinoni L., Johnson S., Kreppel F., Kochanek S., van den Broek M., Radbruch A., Lévy F., Lambert P., Siegrist C., Restifo N. P., Löhning M., Ochsenbein A. F., Nabel G. J., Pinschewer D. D., *Nat. Med.*, **16**, 339—345 (2010).
13) Engelmayer J., Larsson M., Subklewe M., Chahroudi A., Cox W. I., Steinman R. M., Bhardwaj N., *J. Immunol.*, **163**, 6762—6768 (1999).
14) Gao W., Rzewski A., Sun H., Robbins P. D., Gambotto A., *Biotechnol. Prog.*, **20**, 443—448 (2004).
15) Kavanagh D. G., Kaufmann D. E., Sunderji S., Frahm N., Gall S. L., Boczkowski D., Rosenberg E. S., Stone D. R., Johnston M. N., Wagner B. S., Zaman M. T., Brander C., Gilboa E., Walker B. D., Bhardwaj N., *Blood*, **107**, 1963—1969 (2006).
16) Felgner J. H., Kumar R., Sridhar C. N., Wheeler C. J., Tsai Y. J., Border R., Ramsey P., Martin M., Felgner P. L., *J. Biol. Chem.*, **269**, 2550—2561 (1994).
17) Rughetti A., Biffoni M., Sabbatucci M., Rahimi H., Pellicciotta I., Fatorossi A., Pierelli L., Scambia G., Lavitrano M., Frati L., Nuti M., *Gene Ther.*, **7**, 1458—1466 (2000).
18) Li G. B., Li G. X., *Mol. Biotechnol.*, **43**, 250—256 (2009).
19) Ohnishi Y., Fujii H., Hayakawa Y., Sakukawa R., Yamaura T., Sakamoto T., Tsukada K., Fujimaki M., Nunome S., Komatsu Y., Saiki I., *Cancer Sci.*, **89**, 206—213 (1998).
20) Matsuo M., Sakurai H., Koizumi K., Saiki I., *Cancer Lett.*, **251**, 288—295 (2007).
21) Shen Z., Reznikoff G., Dranoff G., Rock K. L., *J. Immunol.*, **158**, 2723—2730 (1997).
22) Felgner P. L., Gadek T. R., Holm M., Roman R., Chan H. W., Wenz M., Northrop J. P., Ringold G. M., Danielsen M., *Proc. Natl. Acad. Sci. U.S.A.*, **84**, 7413—7417 (1984).
23) Malone R. W., Felgner P. L., Verma I. M., *Proc. Natl. Acad. Sci. U.S.A.*, **86**, 6077—6081 (1989).
24) Debs R. J., Freedman L. P., Edmunds S., Gaensler K. L., Düzgünes N., Yamamoto K. R., *J. Biol. Chem.*, **265**, 10189—10192 (1990).
25) Chiang M. Y., Chan H., Zounes M. A., Freier S. M., Lima W. F., Bennett C. F., *J. Biol. Chem.*, **266**, 18162—18171 (1991).
26) Lin M. F., Davolio J., Garcia R., *Biochem. Biophys. Res. Commun.*, **192**, 413—419 (1993).
27) Lee S. J., Lee I. S., Mar W., *Arch. Pharm. Res.*, **26**, 832—839 (2003).
28) Genfa L., Jiang Z., Hong Z., Yimin Z., Liangxi W., Guo W., Ming H., Donglen J., Lizhao W., *Int. Immunopharmacol.*, **5**, 1007—1017 (2005).
29) Zhang J., Li L., Kim S. H., Hagermana A. E., Lü J., *Pharm. Res.*, **26**, 2066—2080 (2009).
30) Kaur G., Athar M., Alam M. S., *Chem. Biol. Interact.*, **171**, 272—282 (2008).
31) Toshkova R., Nikolova N., Ivanova E., Ivancheva S., Serkedjieva J., *Pharmazie*, **59**, 150—154 (2004).
32) Svajger U., Obermajer N., Jeras M., *Immunology*, **129**, 525—535 (2010).
33) Okada N., Saito T., Mori K., Masunaga Y., Fujii Y., Fujita J., Fujimoto K., Nakanishi T., Tanaka K., Nakagawa S., Mayumi T., Fujita T., Yamamoto A., *Biochim. Biophys. Acta-Gen. Subj.*, **1527**, 97—101 (2001).
34) Korsholm K. S., Agger E. M., Foged C., Christensen D., Dietrich J., Andersen C. S., Geisler C., Andersen P., *Immunology*, **121**, 216—226 (2007).
35) Elouahabi A., Ruysschaert J. M., *Mol. Ther.*, **11**, 336—347 (2005).
36) Lee S. M., Li M. L., Tse Y. C., Leung S. C., Lee M. M., Tsui S. K., Fung K. P., Lee C. Y., Waye M. M., *Life Sci.*, **71**, 2267—2277 (2002).
37) Rodriguez A., Regnault A., Kleijmeer M., Icciardi-Castagnoli P., Amigorena S., *Nat. Cell Biol.*, **1**, 362—368 (1999).
38) Luts M. B., Kukutsch N., Ogilvie A. L., Rössner S., Koch F., Romani N., Schuler G., *J. Immunol. Methods*, **223**, 77—92 (1999).
39) Haas J., Park E. C., Seed B., *Curr. Biol.*, **6**, 315—324 (1996).
40) Araki N., Johnson M. T., Swanson J. A., *J. Cell Biol.*, **135**, 1249—1260 (1996)
41) Van Tendeloo V. F., Ponsaerts P., Lardon F., Nijs G., Lenjou M., Van Broeckhoven C., Van Bockstaele D. R., Berneman Z. N., *Blood*, **98**, 49—56 (2001).

42) Nguyen L. T., Atobe K., Barichello J. M., Ishida T., Kiwada H., *Biol. Pharm. Bull.*, **30**, 751—757 (2007).
43) Khalil I. A., Kogure K., Akita H., Harashima H., *Pharmacol. Rev.*, **58**, 32—45 (2006).
44) Cotton M., Längle-Rouault F., Kirlappos H., Wagner E., Mechtler K., Zenke M., Beug H., Birnstiel M. L., *Proc. Natl. Acad. Sci. U.S.A.*, **87**, 4033—4037 (1990).
45) Friend D. S., Papahadjopoulos D., Debs R. J., *Biochim. Biophys. Acta-Biomembr.*, **1278**, 41—50 (1996).
46) Chikh G., Schutze-Redelmeir M. P., *Biosci. Rep.*, **22**, 339—353 (2002).
47) Serre K., Machy P., Grivel J. C., Jolly G., Brun N., Barbet J., Leserman L., *J. Immunol.*, **161**, 6059—6067 (1998).
48) Suzuki R., Utoguchi N., Kawamura K., Kadowaki N., Okada N., Takizawa T., Uchiyama T., Maruyama K., *Yakugaku Zasshi*, **127**, 301—306 (2007).
49) Sallusto F., Cella M., Danieli C., Lanzavecchia A., *J. Exp. Med.*, **182**, 389—400 (1995).
50) Diebold S. S., Plank C., Cotton M., Wagner E., Zenke M., *Somat. Cell Mol. Genet.*, **27**, 65—74 (2002).
51) Li Y., Kim J., Li J., Liu F., Liu X., Himmeldirk K., Ren Y., Wagner T. E., Chen X., *Biochem. Biophys. Res. Commun.*, **336**, 430—437 (2005).
52) Speirs K., Lieberman L., Caamano J., Hunter C. A., Scott P., *J. Immunol.*, **172**, 752—756 (2004).
53) Cejas P. J., Carlson L. M., Zhang J., Padmanabhan S., Kolonias D., Lindner I., Haley S., Boise L. H., Lee K. P., *J. Biol. Chem.*, **280**, 28412—28423 (2005).
54) Cejas P. J., Carlson L. M., Kolonias D., Zhang J., Lindner I., Billadeau D. D., Boise L. H., Lee K. P., *Moll. Cell. Biol.*, **25**, 7900—7916 (2005).
55) Pan M. H., Lin-Shiau S. Y., Ho C. T., Lin J. H., Lin J. K., *Biochem. Pharmacol.*, **59**, 357—367 (2000).
56) Tan P. H., Beutelspacher S. C., Wang Y. H. , McClure M. O., Ritter M. A., Lombardi G., George A. J. T., *Mol. Ther.*, **11**, 790—800 (2005).
57) Curiel-Lewandrowski C., Mahnke K., Labeur M., Roters B., Schmidt W., Granstein R. D., Luger T. A., Schwarz T., Grabbe S., *J. Immunol.*, **163**, 174—183 (1999).
58) Nukiwa M., Andarini S., Zaini J., Xin H., Kanehira M., Suzuki T., Fukuhara T., Mizuguchi H., Hayakawa T., Saijo Y., Nukiwa T., Kikuchi T., *Eur. J. Immunol.*, **36**, 1019—1027 (2006).

JOURNAL OF VIROLOGY, Nov. 2010, p. 11614–11623 Vol. 84, No. 22
0022-538X/10/$12.00 doi:10.1128/JVI.01053-10

CD1d, a Sentinel Molecule Bridging Innate and Adaptive Immunity, Is Downregulated by the Human Papillomavirus (HPV) E5 Protein: a Possible Mechanism for Immune Evasion by HPV[▽]

Shiho Miura,[1] Kei Kawana,[1]* Danny J. Schust,[2] Tomoyuki Fujii,[1] Terufumi Yokoyama,[3] Yuki Iwasawa,[1] Takeshi Nagamatsu,[1] Katsuyuki Adachi,[1] Ayako Tomio,[1] Kensuke Tomio,[1] Satoko Kojima,[1] Toshiharu Yasugi,[1] Shiro Kozuma,[1] and Yuji Taketani[1]

Department of Obstetrics and Gynecology, Faculty of Medicine, University of Tokyo, 7-3-1 Hongo, Bunkyo-ku, Tokyo 113-8655, Japan[1]; Division of Reproductive Endocrinology and Fertility, Department of Obstetrics, Gynecology, and Women's Health, University of Missouri School of Medicine, Columbia Regional Hospital, 402 Keene Street, Third Floor, Columbia, Missouri 65201[2]; and GENOLAC BL Corp. 503, Okinawa Industry Support Center, 1831-1, Oroku, Naha, Okinawa 901-0152, Japan[3]

Received 16 May 2010/Accepted 20 August 2010

CD1d and CD1d-restricted natural killer T (NKT) cells serve as a natural bridge between innate and adaptive immune responses to microbes. CD1d downregulation is utilized by a variety of microbes to evade immune detection. We demonstrate here that CD1d is downregulated in human papillomavirus (HPV)-positive cells *in vivo* and *in vitro*. CD1d immunoreactivity was strong in HPV-negative normal cervical epithelium but absent in HPV16-positive CIN1 and HPV6-positive condyloma lesions. We used two cell lines for *in vitro* assay; one was stably CD1d-transfected cells established from an HPV-negative cervical cancer cell line, C33A (C33A/CD1d), and the other was normal human vaginal keratinocyte bearing endogenous CD1d (Vag). Flow cytometry revealed that cell surface CD1d was downregulated in both C33A/CD1d and Vag cells stably transfected with HPV6 E5 and HPV16 E5. Although the steady-state levels of CD1d protein decreased in both E5-expressing cell lines compared to empty retrovirus-infected cells, CD1d mRNA levels were not affected. Confocal microscopy demonstrated that residual CD1d was not trafficked to the E5-expressing cell surface but colocalized with E5 near the endoplasmic reticulum (ER). In the ER, E5 interacted with calnexin, an ER chaperone known to mediate folding of CD1d. CD1d protein levels were rescued by the proteasome inhibitor, MG132, indicating a role for proteasome-mediated degradation in HPV-associated CD1d downregulation. Taken together, our data suggest that E5 targets CD1d to the cytosolic proteolytic pathway by inhibiting calnexin-related CD1d trafficking. Finally, CD1d-mediated production of interleukin-12 from the C33A/CD1d cells was abrogated in both E5-expressing cell lines. Decreased CD1d expression in the presence of HPV E5 may help HPV-infected cells evade protective immunological surveillance.

There are approximately 100 identified genotypes (types) of human papillomavirus (HPV). Over 40 of these are classified as genital HPV subtypes that invade the reproductive organs, including the uterine cervix, vaginal wall, vulva, and penis. Genital HPV types are further subclassified into high-risk types that are commonly associated with cervical cancer and low-risk types that cause noninvasive condyloma acuminata. Although exact classification varies among researchers, subtypes 16, 18, 31, 33, 35, 39, 45, 51, 52, 56, 58, 66, and 68 are typically classified as high risk and subtypes 6, 11, 40, 42, 43, 44, 54, 61, and 72 as low risk (44). Genital HPV infection involves short-term virus proliferation, followed by the long-term latent presence of a small number of copies of the viral genome within the basal cells of the genital epithelium (44). Infections with high-risk HPV subtypes result in progression to genital tract cancers (most commonly cervical) in only a small percentage of infected women and typically after a long latency period. A high percentage of high-risk HPV DNA-positive infected women resolve their infections during the proliferative phase and thereby clear the virus or progress to latency with undetectable HPV DNA levels. The clearance of viral DNA is often accomplished through activation of the host immune system against viral antigen (19), and chronic immune suppression represents a risk factor for viral DNA persistence and benign and/or neoplastic lesion progression (23).

Completion of the HPV life cycle requires infection of epidermal or mucosal basal cells that have the potential to proliferate and differentiate. Within these cells, overall viral gene expression is suppressed, although limited expression of specific early viral genes, including E5, E6, and E7, causes lateral expansion of infected cells within the basal layer of the epithelium (44). HPV E5 seems to be particularly important early in the course of infection. Large amounts of E5 mRNA have been found in cervical intraepithelial neoplasia (CIN) lesions (37). However, as HPV-infected lesions progress to cervical cancer, episomal viral DNA becomes integrated into host cell DNA, and a substantial part of the HPV genome, commonly including the E5 coding sequence, is deleted (16). Therefore, E5 is not obligatory in the late events of HPV-mediated carcinogenesis.

E5 is a small hydrophobic protein that can be localized within the Golgi apparatus (GA), endoplasmic reticulum

* Corresponding author. Mailing address: Department of Obstetrics and Gynecology, Faculty of Medicine, University of Tokyo, 7-3-1 Hongo, Bunkyo-ku, Tokyo 113-8655, Japan. Phone: 81-3-3815-5411. Fax: 81-3-3816-2017. E-mail: kkawana-tky@umin.ac.jp.

[▽] Published ahead of print on 1 September 2010.

(ER), and occasionally at the plasma membrane of the host cell. It has been proposed that binding of HPV16 E5 to a subunit of the cellular proton ATPase (15) is responsible for the lack of acidification of the GA and endolysosomes and the consequent impaired function of these organelles that is seen with HPV16 infection (32, 38). The presence of HPV16 E5 has also been linked to downregulation of antigen presentation by HLA class I molecules, a process that may aid in HPVs ability to evade immune clearance through cytotoxic-T-lymphocyte (CTL)-mediated adaptive immunity (1, 2, 3, 21, 30). Ashrafi and coworkers have demonstrated that HPV16 E5 retains HLA-A and -B molecules in the GA and interferes with their trafficking to the cell surface but does not alter the transcription of HLA class I heavy chains or the transporter associated with antigen processing (TAP) (2, 3, 4, 28). Others have shown that HPV16 E5 interacts with calnexin in the ER and thereby interferes with the modification of HLA class I heavy chains (21).

CD1d is an major histocompatibility complex (MHC) class I-like glycoprotein that presents self or microbial lipid antigen to natural killer T (NKT) cells (39). In humans, a specific subset of NKT cells expresses an invariant Vα24-JaQ/Vβ11 TCR (iTCR) and can recognize CD1d on the surface of antigen-presenting cells (APCs) through this receptor. CD1d is expressed not only in typical APCs (macrophages, dendritic cells, and B cells) but also in intestinal epithelial cells (8, 12), foreskin keratinocytes (9), and reproductive tract epithelial cells (25, 26). Like MHC class I, CD1d is synthesized, glycosylated by *N*-glycosyltransferase, modified, and assembled with β2m within the ER and then transferred to the GA (5, 24, 27). CD1d plays a role in both innate and adaptive immunity to various bacteria, viruses, fungi, and parasites (reviewed in reference 10). Activation of CD1d-restricted invariant NKT (iNKT) cells enhances host resistance to some microbes in a manner that depends on the level of CD1d expression on APCs (34, 35). In contrast, the activation of iNKT cells promotes susceptibility to some microbes (7, 33). The activation of CD1d-restricted iNKT cells in response to microbial invasion is antigen dependent, but these antigens can be derived from the invading microbe or possibly from host lipids (11, 22, 29). Intracellular signaling mediated by surface CD1d utilizes NF-κB, a well-known immune-related transcription factor (36, 43). CD1d-restricted NKT cells can modulate adaptive immune cells by altering Th1/Th2 polarization. Recognition of CD1d by iNKT cells can also result in rapid release of both interleukin-4 (IL-4) and gamma interferon (IFN-γ) from the NKT cell (6). Therefore, CD1d and CD1d-restricted NKT cells serve as a natural bridge between innate and adaptive immune responses to microbes. Not surprisingly, several microbes, including herpes simplex virus type 1, human immunodeficiency virus, Kaposi's sarcoma herpesvirus, and *Chlamydia trachomatis*, are known to downregulate cell surface expression of CD1d as an immune evasion strategy (13, 26, 31, 42). Our own lab previously demonstrated that *C. trachomatis* retains CD1d in the ER and targets CD1d to both chlamydial and cellular degradation pathways (26).

Viewing the importance of CD1d in innate immune responses to microbes, we hypothesized that HPV may alter CD1d-mediated immune pathways and thereby avoid innate immune destruction of the infected cell by the host. We demonstrate here that the presence of the E5 protein of HPV6 and HPV16 is associated with reduced CD1d cell surface expression. We describe a mechanism for this downregulation and hypothesize that decreased surface CD1d expression may help HPV-infected cells evade immune surveillance during the early stages of infection.

MATERIALS AND METHODS

HPV6 and HPV16 E5 expression constructs. HPV6 and HPV16 E5 open reading frames were amplified from the HPV6 and HPV16 complete genomes (kindly provided by Tadahito Kanda, National Institute of Infectious Diseases, Japan) by PCR using primers designed to introduce BamHI (forward) and EcoRI (reverse) restriction sites. The PCR products were digested with BamHI and EcoRI and subcloned into a retroviral expression plasmid pLPCX (Clontech, Mountain View, CA).

Cell lines and establishment of a cell line stably expressing CD1d. An HPV-negative human cervical carcinoma cell line, C33A, and a vaginal epithelial cell that was originally established from normal human primary epithelial cells that were immortalized by transduction with HPV16 E6/E7 genes (VK2/E6E7) (a generous gift from D. J. Anderson, Boston University, Boston, MA) (18) were grown in Dulbecco modified eagle medium (Invitrogen, Carlsbad, CA) without $CaCl_2$ (Invitrogen), supplemented with 10% fetal bovine serum (Invitrogen) at 37°C in 5% CO_2. The vaginal epithelial (VK2/E6E7) cells used here are known to express endogenous CD1d at the cell surface (25).

A CD1d-expressing retroviral plasmid pSRα-neo (kindly provided by R. Blumberg, Harvard Medical School, Boston, MA) was transfected into Phoenix cells, a packaging cell line for recombinant retroviruses (kindly provided by K. Oda, University of Tokyo), using Lipofectamine 2000 (Invitrogen). After 72 h of incubation in DMEM, the culture medium containing released CD1d-expressing retroviruses was collected and used to infect C33A cells and transfer the CD1d gene. CD1d-expressing C33A cells were selected in medium containing 1.0 mg of neomycin/ml to establish a stably transfected cell line (C33A/CD1d).

Establishment of HPV E5-expressing cell lines. HPV6 or HPV16 E5-expressing retroviral plasmids or their empty counterparts (pLPCX-16E5, pLPCX-6E5, or pLPCX, respectively) were transfected into Phoenix cells using Lipofectamine 2000 (Invitrogen). After 72 h of incubation, culture medium with released viruses were collected and used to infect C33A/CD1d or vaginal epithelial cells. Stable cell lines were selected in media containing 1.5 μg of piromycin/ml.

Immunohistochemistry. Immunostaining for CD1d was performed on formalin-fixed, paraffin-embedded tissue sections of normal or inflamed cervix, CIN1 to CIN3, cervical cancer, and condyloma acuminata (obtained under IRB approval through the University of Tokyo). A total of 45 tissues were examined. Optimal immunostaining required antigen retrieval via microwave exposure in 0.01 M citrate buffer. A mouse anti-CD1d MAb (NOR3.2, 1:100; Abcam, Inc., Cambridge, MA) or an irrelevant, isotype-matched mouse monoclonal antibody (DakoCytomation, Glostrup, Denmark) were used as primary reagents. Immunostaining was amplified and detected by using the EnVision+System-HRP (DakoCytomation). Nuclei were counterstained by using standard hematoxylin protocols (Sigma-Aldrich, Inc., St. Louis, MO). Analyses were performed at a magnification of ×200.

Flow cytometry. C33A/CD1d cells were grown in 175-cm^2 flasks until confluent, harvested using trypsin-EDTA, and pelleted at 500 × *g* for 5 min at room temperature. The cells were then washed and resuspended in PBS-B (phosphate-buffered saline [PBS] with 1% bovine serum albumin; Invitrogen) at a concentration of 10^6 cells/ml. For detection of cell surface CD1d, 100 μl of cell suspension was incubated with an anti-CD1d NOR3.2 monoclonal antibody (MAb; Abcam) at 1:100 for 30 min at 4°C. Cells were then washed three times in PBS-B, incubated with a goat anti-mouse immunoglobulin secondary antibody conjugated to phycoerythrin (PE; BD Bioscience, San Jose, CA) for 30 min at 4°C, suspended in 1% paraformaldehyde, and analyzed by using a FACSCalibur flow cytometry system (BD Bioscience).

Proteasome inhibitor treatment. C33A/CD1d cells harboring an empty vector (C33A/CD1d-empty) or expressing HPV6 E5 (C33A/CD1d-6E5) or HPV16 E5 (C33A/CD1d-16E5) were cultured for up to 24 h in the presence or absence of the cytosolic proteasome inhibitor MG132 (10 μM in dimethyl sulfoxide [DMSO]; Sigma-Aldrich, Inc.). Control wells included vehicle alone.

HPV genotyping. DNA was extracted from cervical smear samples by using the DNeasy blood minikit (Qiagen, United Kingdom). HPV genotyping was performed by using the PGMY-CHUV assay method (20). Briefly, standard PCR was conducted using the PGMY09/11 L1 consensus primer set and HLA-dQ primer sets (20). Reverse blotting hybridization was performed as described

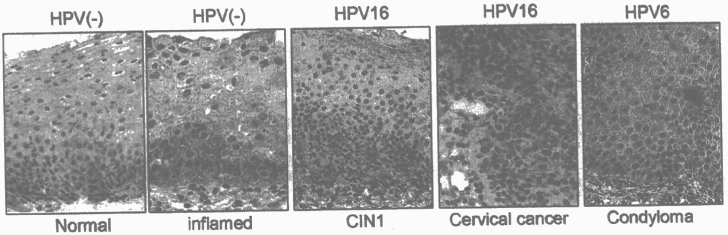

FIG. 1. Immunostaining of HPV-associated lesions for CD1d. Immunostaining for CD1d was performed after antigen retrieval on formalin-fixed, paraffin-embedded tissue sections of HPV-negative normal and inflamed ectocervical epithelium, HPV16-positive CIN1, HPV16-positive cervical cancer, and HPV6-positive condyloma acuminata. CD1d was detected with NOR3.2, a CD1d-specific MAb (1:100).

previously (20). Heat-denatured PCR amplicons were hybridized to a negatively charged nylon membrane containing specific probes for 32 HPV genotypes and HLA-dQ reference samples. Chemiluminescence detection used enhanced chemiluminescence (ECL) detection reagents for nucleic acids (GE Healthcare). Films were interpreted using the HPV reference guide provided.

RT-PCR and quantitative PCR. Portions (1 μg) of total RNA and oligo(dT)s were used for reverse transcriptase (RT) reactions (RNA PCR kit; Applied Biosystems, Foster City, CA). Total cDNA reaction samples were used as templates for amplification of each gene fragment using a PCR Core kit (Applied Biosystems). Primer pair sets for CD1d were synthesized by Invitrogen (CD1d, 453 bp; 5′-GCTGCAACCAGGACAAGTGGACGAG-3′ [forward] and 5′-AGGAACAGCAAGCACGCCAGGACT-3′ [reverse]). Those for IL-12 p40 were commercially available (Sigma-Aldrich, Inc.). For quantitative PCR, cDNA were produced via RT of 1 μg of total RNA extracted from the cells as described above by using an OmniScript RT kit (Qiagen, Inc., Valencia, CA). Portions (2 μl) of 5-fold-diluted cDNA aliquots were amplified in a thermal cycler (7300 Real-Time PCR System; Applied Biosystems) by using a QuantiTect SYBR green PCR kit (Qiagen, Inc.) and a primer pair set for β-actin (5′-GAAATCGTGCGTGACATTAAGG-3′[forward] and 5′-TCAGGCAGCTCGTAGCTTCT-3′ [reverse]). The mRNA levels for IL-12 were normalized to those of β-actin, the internal control.

Fluorescent deconvolution microscopy and confocal microscopy. C33A/CD1d cells were seeded onto coverslips. The ER was visualized using the ER tracker Blue-White DPX (Invitrogen) for 30 min at 37°C. All coverslips were fixed in 4% paraformaldehyde, permeabilized with 0.1% Tween 20. They were then incubated for 1 h at 37°C with either an anti-CD1d NOR3.2 MAb labeled with Zenon Alexa Fluor 555 using a mouse IgG labeling kit (Invitrogen) or an anti-FLAG MAb labeled with Zenon Alexa Fluor 488 using a mouse IgG labeling kit (Invitrogen) singly or in combination. With the exception of ER tracker-treated coverslips, the cells were then counterstained with a DAPI (4′,6′-diamidino-2-phenylindole) nucleic acid stain (Invitrogen). Images were obtained with a LSM 700, flexible confocal microscope (Carl Zeiss, Oberkochen, Germany). Filter sets were optimized for Alexa 488, Alexa 555, and DAPI. Z-axis plane capture, deconvolution, and analyses were performed with ZEN 2009 Software (Carl Zeiss).

Western blotting. Portions (50 μg) of total cell lysates from C33A/CD1d-empty, C33A/CD1d-6E5, or C33A/CD1d-16E5 cells in a modified TNF buffer (1 M Tris-HCl [pH 7.8], 10% NP-40, 5 M NaCl, 0.5 M EDTA [pH 8.0], aprotinin, 0.1 M phenylmethylsulfonyl fluoride) were electrophoresed and transferred to nitrocellulose membranes. Membranes were blocked with 10% milk and incubated with a peroxidase-labeled anti-CD1d NOR3.2 MAb (1:200; Abcam) or an anti-FLAG MAb (1:500; Sigma-Aldrich, Inc.) using a peroxidase labeling kit (Roche, Basel, Switzerland) for 1 h. Membranes were washed and bound antibody was detected using an ECL Western blotting analysis system (GE Healthcare Buckinghamshire, United Kingdom).

Immunoprecipitation and Western immunoblotting. Harvested C33A/CD1d-empty, C33A/CD1d-6E5, or C33A/CD1d-16E5 cells were lysed in modified radioimmunoprecipitation assay buffer (1% NP-40, 1% deoxycholate, 0.1% sodium dodecyl sulfate [SDS], 10 mM Tris, 150 mM NaCl, 2 mM EDTA) with protease inhibitors (Amersham Biosciences, Piscataway, NJ). Equivalent aliquots of total cell lysates were incubated overnight at 4C with 5 μg of mouse anti-FLAG MAbs (Sigma-Aldrich, Inc.)/ml and 5 μl of protein A-Sepharose (GE Healthcare). Precipitated proteins were separated by SDS-PAGE using 7.5% acrylamide gels and transferred to polyvinylidene difluoride membranes. Mouse anti-calnexin or rabbit anti-β-actin polyclonal antibodies (Abcam) were used as primary reagents for immunoblotting, and anti-mouse IgG-HRP (1:100,000; GE Healthcare) was used as a secondary reagent. Products in Western immunoblotting experiments were visualized by using an ECL Western blotting analysis system (GE Healthcare). Molecular masses were confirmed by comparison to standard size markers (GE Healthcare).

Statistical analysis. Quantitative PCR data were presented as means ± the standard deviations. Experiments were performed independently at least three times. The Cochran-Armitage Trend test was computed to show trends in immune reactivity with NOR3.2 MAb in clinical samples. IL-12 mRNA levels were compared to those before or after cross-linking by using paired, two-tailed Student *t* tests. A P value of <0.05 was considered significant.

RESULTS

CD1d downregulation in HPV-related lesions and cancer cell lines. Since CD1d expression in human mucosa and skin has been demonstrated by immunohistochemistry using the anti-CD1d NOR3.2 MAb (2, 9, 12, 26), we examined immunostaining of human normal ectocervix or HPV-related lesions with NOR3.2 (Fig. 1). Immunostaining for CD1d was performed on formalin-fixed, paraffin-embedded tissue sections of normal or inflamed ectocervical epithelium, cervical intraepithelial neoplasia 1 (CIN1), cervical cancer, and cervical condyloma (obtained under IRB approval through the University of Tokyo, Faculty of Medicine). To examine alterations in CD1d expression in the presence of high-risk HPV and low-risk HPV subtypes, HPV16-positive CIN1 or cancer lesions and HPV6-positive condyloma acuminata specimens were compared to each other and to HPV-negative normal and inflamed ectocervical epithelial controls. Immunoreactivity with the NOR3.2 MAb was noted in the basal and parabasal epithelial cells of normal and inflamed ectocervical epithelia that are known to express early HPV genes (E5, E6, and E7; Fig. 1) (44). In inflamed epithelium, the immunoreactivity appeared to be intensified compared to normal epithelium. CD1d expression is known to be enhanced by inflammatory cytokines (10). NOR3.2 immunoreactivity is essentially absent in HPV16-positive CIN1, HPV16-positive cancer, and HPV6-positive condyloma lesions (Fig. 1). To statistically analyze alterations in CD1d expression, a total of 45 clinical specimens from normal controls and HPV-related lesions were immunostained with NOR3.2 (Table 1). NOR3.2 immunoreactivity was

TABLE 1. Immunoreactivity with NOR3.2 anti-CD1d MAb in cervical epithelium of various lesions

Histological status	HPV status[a]	CD1d (no. of cases)		% Positive[b]
		Positive	Negative	
Normal/inflamed		9	1	90.0
CIN1 and CIN2	HR-HPV(+)	0	7	0
CIN3	HR-HPV(+)	2	16	11.1
Cancer	HR-HPV(+)	0	7	0
Condyloma	HPV6(+)	0	3	0

[a] HR-HPV(+), any high-risk HPV positive.
[b] $P = 0.0001$ (exact Cochran-Armitage Trend test).

mostly limited to the HPV-negative normal or inflamed ectocervical epithelial samples similar to those represented in the first two panels of Fig. 1. NOR3.2 immunoreactivity was absent in all CIN1 and CIN2, cervical cancer, and condyloma lesions. Among CIN3 samples, two lesions showed NOR3.2 immunoreactivity, whereas 16 lesions did not. Using trend analysis, we were able to demonstrate an association between decreased CD1d immunoreactivity and progression of cervical neoplastic lesions with statistical significance ($P = 0.0001$).

Although HPV E5 is not expressed in cervical cancer cells (16), immunohistochemical data demonstrated that CD1d expression was also abrogated in cervical cancer lesions. To address the mechanisms underlying CD1d downregulation in cervical cancers, we examined the level of CD1d transcription and CD1d expression at the cell surface in several cervical cancer cell lines (Fig. 2). As a positive control, we created cell transfectants that stably expressed CD1d. To avoid the potential influence of endogenous HPV protein expression, an HPV-negative cervical cancer cell line, C33A, was used for our CD1d transfectants. We used a retrovirus vector to transduce the CD1d gene into these cells and established the stable cell line, C33A/CD1d via neomycin selection. Flow cytometry revealed strong expression of CD1d on the cell surface of C33A/CD1d cells. Cd1d was not expressed on the cell surface of C33A control cells or in other cancer cell lines (Fig. 2A). To examine the level of CD1d transcription in these same cells, cDNA was produced via RT of total RNA from each cell line and subjected to PCR using primer pairs specific for CD1d. The expected single band representing CD1d was observed on agarose gels only in C33A/CD1d cells (Fig. 2B). These data indicated that CD1d expression was abrogated prior to or during transcription the tested cervical cancer cell lines.

Cell surface expression of CD1d decreases in HPV E5-expressing epithelial cells. HPV E5 has been reported to inhibit cell surface expression of HLA class I molecules by interfering with their trafficking to the cell surface (1, 2, 3, 21, 30). Since CD1d and HLA class I heavy chains utilize an identical intracellular pathway to traffic from the ER to the cell surface, we hypothesized that HPV E5 may also interfere with surface CD1d expression at a posttranscriptional level. To verify our immunohistochemical data and study CD1d trafficking in the presence of E5 *in vitro*, we created HPV6 and HPV16 E5 stably transfected cell lines using C33A/CD1d cells. Since the E5 protein is less than 10 kDa in size, the production of an anti-E5 antibody would be difficult. Instead, E5 proteins were tagged with FLAG and detected by Western blotting or immunostaining with an anti-FLAG antibody. FLAG-tagged HPV6 or HPV16 E5 genes were transduced into the C33A/CD1d cells by using retrovirus vectors. To control for the influence of retrovirus infection and the presence of the expression vector, C33A/CD1d cells were infected with empty retrovirus vectors. Retrovirus-infected cells were exposed to puromycin, and E5-expressing C33A/CD1d cells were established (C33A/CD1d-6E5, -16E5, and -empty). In Fig. 3A, lanes 5 and 6, show PCR products derived from cDNA generated by RT of total RNA from C33A/CD1d-6E5 and -16E5 cells. Lanes 2 and 3 in the same figure show PCR products derived from corresponding expression plasmid DNA. FLAG-6E5 and -16E5 were transcribed in C33A/CD1d-6E5 and -16E5 cells, respectively. Using Western immunoblotting and an anti-FLAG MAb, FLAG-6E5 and -16E5 proteins were detected as immunoreactive bands at an approximate size of 10 kDa in lanes 1 and 2, respectively (Fig. 3B).

We next examined the expression of CD1d at both mRNA and protein levels in the presence or absence of HPV E5. CD1d transcription levels in C33A/CD1d cells were unaffected by the presence of E5 or of empty vector compared to naive

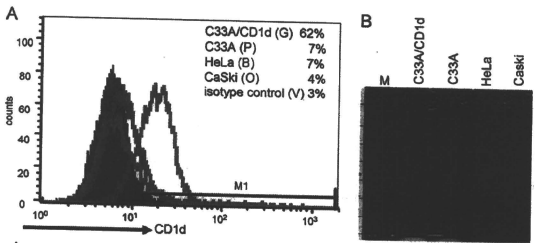

FIG. 2. CD1d alterations in cancer cell lines. (A) Cell surface expression of CD1d in C33A (pink line), HeLa (blue line), CaSki (orange line), and C33A/CD1d (green line) cells. All cells were stained with an anti-CD1d primary MAb (NOR3.2; 1:100 dilution) and a PE-conjugated goat anti-mouse immunoglobulin secondary antibody (1:20 dilution). Background staining of the cells using an isotype-matched control antibody is also shown (filled region). Cells were suspended in 1% paraformaldehyde and analyzed by using a FACSCalibur flow cytometry system. (B) Transcription of CD1d. cDNA was produced via RT of 1 μg of total RNA from each cell line and amplified by PCR with primer pairs specific for CD1d. PCR products were separated over an agarose gel containing ethidium bromide.

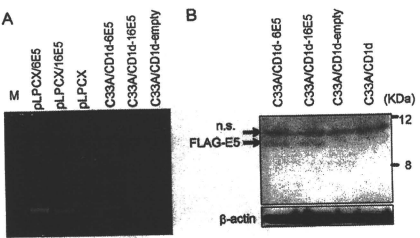

FIG. 3. HPV E5 detection in HPV E5-transformed C33A/CD1d cells. (A) Transcription of HPV E5. cDNA was produced via RT of 1 μg of total RNA from each cell line and amplified by PCR with primer pairs specific for HPV16 E5 and HPV6 E5. PCR products were separated over an agarose gel containing ethidium bromide. Lanes 5 and 6 display PCR products derived from C33A/CD1d-6E5 and -16E5 cDNA, respectively, while lanes 2 and 3 show PCR products derived from corresponding expression plasmid DNA. Lanes 4 and 7 represent negative control plasmid and cell lines lacking E5, respectively. (B) Translation of HPV E5. Fifty-microgram aliquots of protein lysates from each cell line were analyzed by Western immunoblotting with antibodies against the FLAG tag (1:500 dilution) and β-actin (loading control).

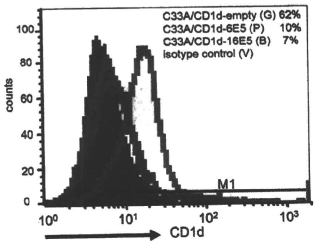

FIG. 5. Cell surface expression of CD1d in C33A/CD1d-empty (green line), C33A/CD1d-6E5 (pink line), and -16E5 (blue line) cells. All cells were stained with an anti-CD1d primary MAb (NOR3.2; 1:100 dilution) and a PE-conjugated goat anti-mouse immunoglobulin secondary antibody (1:20 dilution). Background staining of the cells with an isotype-matched control antibody is also shown (filled region). Cells were suspended in 1% paraformaldehyde and analyzed using a FACSCalibur flow cytometry system.

C33A/CD1d cells (Fig. 4A). In contrast, the 48-kDa, mature glycosylated form of the CD1d heavy chain (HC) that was detected in naive C33A/CD1d and C33A/CD1d-empty cells was completely abrogated in C33A/CD1d-6E5 and barely detectable in the C33A/CD1d-16E5 cells (Fig. 4B, lanes 1, 4, 2, and 3, respectively). The presence of HPV6 and HPV16 E5 drastically inhibited the maturation of CD1d HCs. Flow cytometry was used to analyze the effect of HPV E5 on cell surface expression of CD1d in the C33A/CD1d cells harboring E5-expressing or empty vector (Fig. 5). CD1d was expressed by the majority of C33A/CD1d-empty cells but absent in >70% of C33A/CD1d-6E5 or -16E5 cells (Fig. 5).

To confirm the effect of E5 on endogenous CD1d, we used a vaginal epithelial cell line immortalized via HPV16 E6/E7 transduction of primary cells collected from normal human vaginal epithelium and subsequently well characterized as possessing histological and immunological characteristics identical to those of primary epithelial cells (18). We have previously reported the endogenous expression of functional CD1d molecules on the surface of these cells (25). Since vaginal epithelial cells are well-known targets of genital HPV, these cells were considered to be useful as an *in vitro* model for *in vivo* HPV infections. FLAG-tagged HPV6 or HPV16 E5 genes were transduced into these vaginal cells by using retrovirus vectors (Vag-6E5 and -16E5). We then examined the expression of CD1d at various levels in the presence or absence of HPV E5 (Fig. 6). RT-PCR and Western blotting revealed that CD1d transcription was unaffected by the presence of E5, but the 48-kDa CD1d HC product clearly decreased in Vag-6E5 and -16E5 cells compared to naive and Vag-empty cells (Fig. 6A). Flow cytometry confirmed the decreased cell surface expression of CD1d in 6E5-expressing vaginal epithelial cells (Fig. 6B).

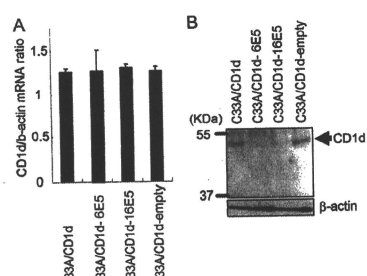

FIG. 4. CD1d heavy-chain transcription and translation in C33A/CD1d, C33A/CD1d-empty, C33A/CD1d-6E5, and C33A/CD1d-16E5 cells. (A) Transcription of CD1d HC. The mRNA levels of CD1d were analyzed by quantitative RT-PCR using SYBR green methodology. CD1d mRNA levels were normalized to β-actin. (B) Fifty-microgram aliquots of protein lysates from each cell line were analyzed by Western immunoblotting with a peroxidase-labeled anti-CD1d NOR3.2 MAb (1:200 dilution) and a β-actin loading control.

E5-expressing epithelial cells retain CD1d in the ER. To demonstrate the intracellular localization of CD1d heavy chains in C33A/CD1d cells harboring HPV-6E5 and -16E5, immunofluorescence confocal microscopy was performed with an anti-CD1d MAb (NOR3.2) combined with either an anti-FLAG MAb that detects FLAG-E5 proteins, an ER-specific marker (ER tracker) or DAPI (Fig. 7). In C33A/CD1d-empty control cells, dual labeling for CD1d and the nucleus (DAPI) verified that CD1d could be detected in a diffuse pattern throughout the intracellular space, with increased accumulation near the cell surface but not in the perinuclear area (Fig. 7, upper image). In contrast, decreased amounts of CD1d could be detected in C33A/CD1d-6E5 and -16E5 cells and CD1d proteins were localized to perinuclear areas near the ER. CD1d and ER signals merged in perinuclear areas (pink

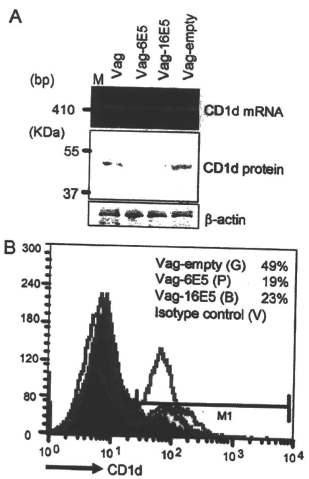

FIG. 6. CD1d downregulation in alternate genital keratinocytes in the presence of 6E5 and 16E5. (A) HPV6 and HPV16 E5 genes were transduced into vaginal epithelial cells established from normal human vaginal epithelium (17) and named Vag-6E5 and Vag-16E5, respectively. PCR products derived from cDNA generated by reverse transcription using 1 μg of total RNA from each of the vaginal cell lines were separated over an ethidium bromide-containing agarose gel. Fifty-microgram aliquots of protein lysates from each vaginal cell line were analyzed by Western immunoblotting with a peroxidase labeled anti-CD1d NOR3.2 MAb (1:200 dilution) and a β-actin loading control. (B) Vag-empty (green line), Vag-6E5 (pink line), and Vag-16E5 (blue line) were stained with an anti-CD1d primary MAb (NOR3.2; 1:100 dilution) and a PE-conjugated goat anti-mouse immunoglobulin secondary antibody (1:20 dilution). Background staining of the cells using an isotype-matched control antibody is also shown (filled region). Cells were suspended in 1% paraformaldehyde and analyzed by using a FACSCalibur flow cytometry system.

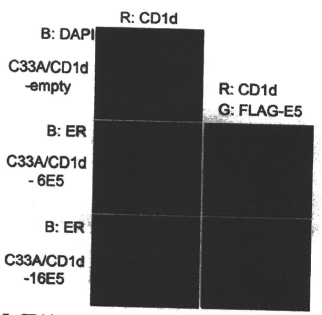

FIG. 7. CD1d trafficking in the presence or absence of E5. C33A/CD1d-empty, C33A/CD1d-6E5, or C33A/CD1d-16E5 cells were seeded onto coverslips. All of the cells were immunostained with an anti-CD1d MAb (NOR3.2, red). C33A/CD1d-empty were also exposed to DAPI (blue), and C33A/CD1d-6E5 or -16E5 cells were exposed to ER tracker (blue) and an anti-FLAG MAb (green). Cells were then visualized by using fluorescence confocal microscopy. Orange to yellow signals represent colocalization of CD1d and E5 within the ER.

signals), suggesting that the majority of CD1d is within the ER (Fig. 7, images on the left). Dual labeling for CD1d and FLAG-E5 verified the colocalization of CD1d and E5 within the ER (orange to yellow signals), while nonmerged FLAG-E5 signals were present in the perinuclear area (pure green), suggesting the presence of E5 in the GA in the absence of CD1d (Fig. 7, images on the right). The results of immunofluorescence microscopy support our biochemical and flow cytometry data showing that mature CD1d protein levels decrease and CD1d fails to traffic to the cell surface in HPV E5-expressing cells.

HPV E5 interacts with calnexin in the ER. Previous biochemical studies have reported that HPV16 E5 interacts with calnexin and that these interactions interfere with the modification of HLA class I heavy chains that typically occurs in the ER (21). The role of calnexin and/or calreticulin in the formation of the second disulfide bond of CD1d HCs in the ER is well described (24). We therefore hypothesized that E5 interacts with calnexin in the ER and may impair calnexin-mediated CD1d folding. This, in turn, could interrupt appropriate trafficking of CD1d to the surface of HPV-infected cells. To address the hypothesis, we examined the interaction of E5 with calnexin using immunoprecipitation. Total cell lysates obtained from C33A/CD1d-empty, -6E5, and -16 E5 cells were incubated with anti-FLAG MAb conjugated beads. FLAG-E5-bound proteins were immunoprecipitated and analyzed by immunoblotting with an anti-calnexin MAb. A band with an apparent molecular mass of 90 kDa and corresponding to calnexin was detected in C33A/CD1d-6E5 and -16 E5 cells, but not C33A/CD1d-empty cells, biochemically demonstrating interaction between E5 with calnexin (Fig. 8A).

To visually demonstrate the colocalization of CD1d and calnexin, C33A/CD1d-empty, -6E5, and -16E5 cells were dually stained with anti-CD1d NOR3.2 and anti-calnexin MAbs and examined by using confocal microscopy. Again, NOR3.2-reactive CD1d was detected throughout the intracellular space in C33A/CD1d-empty cells. In contrast, the majority of CD1d molecules in C33A/CD1d-6E5 or -16E5 cells localized to the perinuclear area (Fig. 8B, images on left). Calnexin detection was rendered as green signals. These mostly localized to perinuclear areas in E5-expressing cells and correspond to the location of ER (Fig. 8B, center images). Although some merge images (yellow signals) could be detected in each cell line, the merge patterns differed between C33A/CD1d-empty and E5-expressing cells (Fig. 8B, images on the right). In C33A/CD1d-empty cells, the calnexin and CD1d signals were mostly distinct and but those that did colocalize appeared to follow the synthetic pathway for type I proteins. In contrast, CD1d in the E5-expressing cells completely colocalized with calnexin, confirming our biochemical data demonstrating physiologic interaction between calnexin and CD1d in the C33A/CD1d-6E5 and -16E5 cells.

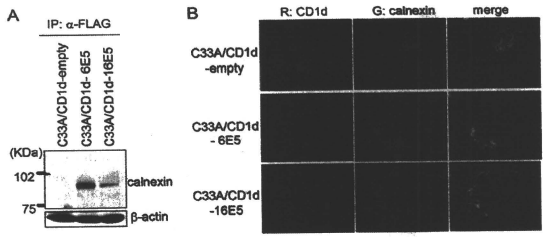

FIG. 8. CD1d and calnexin have direct interactions and colocalize in the perinuclear area in the presence of HPV E5. (A) Protein lysates from C33A/CD1d-empty, C33A/CD1d-6E5, and C33A/CD1d-16E5 cells were immunoprecipitated with an anti-FLAG MAb. Immunoprecipitants were then separated by SDS-PAGE and immunoblotted with an anti-calnexin antibody. (B) C33A/CD1d-empty, C33A/CD1d-6E5, or C33A/CD1d-16E5 cells were seeded onto coverslips. All cells were exposed to an anti-CD1d MAb (NOR3.2, red) and to an anti-calnexin MAb (green) labeled with Zenon Alexa Fluor 488 using a mouse IgG labeling kit. Cells were then visualized by using fluorescence confocal microscopy. Yellow images represent colocalization of CD1d and calnexin.

CD1d was rescued by treatment of proteasome inhibitor. We have previously demonstrated that surface expression of CD1d in human genital epithelial cells is downregulated by *C. trachomatis* infection and that downregulation involves chlamydial protein-mediated proteasomal pathways (26). We hypothesized that HPV infection could utilize posttranslational cellular proteasomal degradation to inhibit cell surface expression of CD1d HC. To address the role of the cellular proteasome in E5-associated CD1d degradation, C33A/CD1d-empty, -6E5, or -16E5 cells were exposed to the proteasome inhibitor, MG132, and CD1d HC levels in cell lysates compared to those in unexposed cells (Fig. 9). Using the NOR3.2 MAb for immunoblotting, the reduced or abrogated expression of the 48-kDa mature CD1d HC in E5-expressing cells could be rescued by the presence of MG132 (Fig. 9A). To visually replicate this effect, immunofluorescence microscopy was performed with the NOR3.2 MAb and DAPI in MG132 exposed and unexposed E5-expressing and control cells (Fig. 9B). In C33A/CD1d-empty cells, NOR3.2-reactive CD1d was detected throughout the intracellular space (Fig. 9B, upper left image). In contrast, NOR3.2-reactive CD1d was barely detected or undetectable in the majority of unexposed C33A/CD1d-6E5 or -16E5 cells (Fig. 9B, upper, right two images). In the presence of proteasomal inhibition with MG132, E5-expressing cells again show CD1d signals throughout the intracellular space (Fig. 9B, lower panels). HPV E5-expressing cells completely recover their expression mature CD1d molecules upon inhibition of cellular proteasomal degradation.

HPV E5 abrogates CD1d-mediated cytokine production in the epithelial cells. Surface CD1d interacts specifically with iNKT cells bearing an iTCR. The interaction not only activates NKT cells but also induces phosphorylation of CD1d, intracellular signaling, and the release of cytokines from the CD1d-bearing cell. We have previously demonstrated that human reproductive tract epithelial cells expressing CD1d on their cell surfaces have the capacity to produce cytokines, especially IL-12, after CD1d ligation (25). IL-12 is a central mediator in both innate and adaptive immunity and is crucial in the prevention of many infectious diseases and tumors (40). IL-12 induces IFN-γ-producing NK, NKT, T helper, and cytotoxic T cells. Since our investigations had demonstrated a decrease in cell surface expression of CD1d in the presence of HPV and specifically of HPV E5, we next examined whether CD1d-mediated IL-12 production was abrogated in E5-expressing epithelial cells (Fig. 10). An anti-CD1d 51.1 MAb can be used for CD1d cross-linking and represents an *in vitro* model for

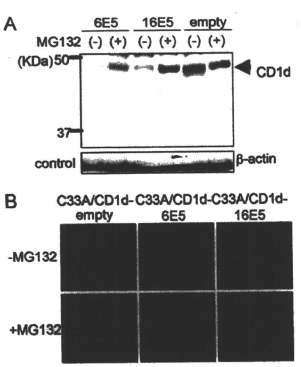

FIG. 9. Proteasome inhibition rescues CD1d from E5-mediated degradation. (A) C33A/CD1d-empty, C33A/CD1d-6E5, or C33A/CD1d-16E5 cells were cultured for up to 24 h in the presence or absence of the cytosolic proteasome inhibitors MG132 (10 μM) in DMSO. Fifty micrograms of protein lysates from each cell line were analyzed by Western immunoblotting with a peroxidase-labeled anti-CD1d MAb (NOR3.2; 1:200 dilution) and a β-actin loading control. (B) C33A/CD1d-empty, C33A/CD1d-6E5, or C33A/CD1d-16E5 cells were seeded onto coverslips and cultured for up to 24 h in the presence (lower) or absence (upper) of MG132 (10 μM) in DMSO. All coverslips were fixed in 4% paraformaldehyde, permeabilized with 0.2% Triton-X, blocked with 6% BSA, and incubated for 1 h at room temperature with an anti-CD1d NOR3.2 MAb (red) directly conjugated with Zenon Alexa Fluor 555 using a mouse IgG1 labeling kit. Cells were then counterstained with a DAPI (blue) nucleic acid stain.

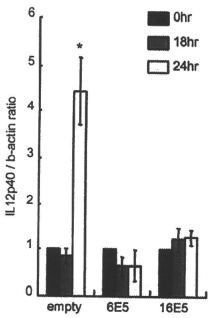

FIG. 10. Autocrine cytokine production upon CD1d cross-linking in C33A/CD1d-empty, C33A/CD1d-6E5, and C33A/CD1d-16E5 cells. An anti-CD1d 51.1 MAb was added at a dosage of 10 μg/ml to cultured epithelial cell monolayers, followed by incubation for 1 h. After being washed with PBS, 10 μg of a goat anti-mouse immunoglobulin antibody/ml was added as a cross-linker for 30 min. The cells were incubated in serum-free growth medium without any antibiotics for 0 to 24 h. cDNA was produced via reverse transcription of 1 μg of total RNA extracted and amplified by PCR with primer pairs for IL-12 p40 and β-actin. IL-12 p40 mRNA levels were normalized to β-actin. Mean values with standard deviations are presented. Asterisks indicate the comparisons (before versus after cross-linking) with statistical significance ($P < 0.05$; $n = 4$).

CD1d ligation (14, 43). C33A/CD1d-empty, -6E5, or -16E5 cells were first exposed to an anti-CD1d 51.1 MAb and then to a secondary anti-mouse IgG cross-linker and then examined for IL-12 production (Fig. 10). IL-12 p40 transcription increased 24 h after cross-linking in the C33A/CD1d-empty cells. This effect was abrogated completely in E5-expressing cells. Decreased cell surface expression of CD1d in E5-expressing cells inhibits the ability of antibodies to cross-link CD1d and thereby halts the downstream signaling that drives IL-12 production.

DISCUSSION

In this study, we attempted to elucidate a mechanism to explain our finding that CD1d was expressed at lower levels in tissues infected with high-risk and low-risk HPV subtypes (16 and 6, respectively). The CD1d protein levels were lower, but the mRNA levels were unaffected in HPV E5-expressing cells, indicating that CD1d is downregulated at a posttranscriptional level in the presence of HPV E5. Modification of CD1d was interrupted at the level of the ER by interactions between HPV E5 and calnexin. Improper folding and/or ubiquitination of CD1d HC in the presence of HPV then targets CD1d to cellular proteasomal degradation. Others (21) have previously demonstrated that interaction of E5 with calnexin appears to interfere with calnexin-assisted folding of HLA class I molecules. Like the well-described quality control system assuring proper HLA class I HC production and maturation, delayed exit of improperly folded CD1d HC from the ER in the presence of HPV E5 appears to result in movement of CD1d HC to the cytosol and cellular proteasomal degradation of CD1d HC via the unfolded protein response. Finally, we addressed the possible functional significance of CD1d degradation in HPV-infected cells. Decreased cell surface expression of CD1d in the presence of HPV 6E5 and 16E5 completely blocked the secretion of IL-12 in response to CD1d cross-linking. Although several of the assays were not quantitative, the effects of HPV6 and HPV16-derived E5 were similar in all assays and were not statistically different in those that were quantitative. This suggests that a mechanism for immune evasion used in the early phase of HPV infection may be conserved between low-risk and high-risk HPV subtypes.

In planning for these investigations, we chose to use two cell lines. One was a cervical cancer cell line that is unique in being HPV-negative C33A. The other was an endogenous CD1d-bearing keratinocyte cell line established from normal human vaginal epithelial cells. The HPV-negative C33A cell was particularly useful for this study because it allowed us to control for the influence on CD1d of proteins other than E5 that could have been potentially present in an HPV-positive cervical cell line. Via transfection, CD1d could be stably expressed in a cervical cell, and specific HPV proteins could added in isolation to assess their effect on CD1d. Our previous and current immunohistochemical data demonstrated that cells in the basal and parabasal cell layers of a variety of squamous genital epithelia react strongly with anti-CD1d MAbs, in patterns that replicate those seen in normal human skin (9, 25). The distribution of CD1d-bearing epithelial cells within the basal and parabasal cell layers may be required for effective interactions between CD1d and the iNKT cells that reside within submucosal tissues. These interactions may occur primarily through CD1d expressed on the basilar membrane. The immortalized vaginal epithelial cell lines used in the present study have been characterized by Fichorova et al. as being similar to epithelial cells present in basal or parabasal cell layers *in vivo* (17, 18). We have also seen similar patterns of CD1d expression in nondiseased genital tract tissues (25). The data derived from vaginal epithelial cells in the present study allowed us to mimic *in vivo* infection of normal human keratinocytes by HPV and to confirm that the retrovirus vectors used to transduce E5 genes into our cell models did not affect the endogenous CD1d promoter.

CD1d transcription was barely detectable in both C33A cells and HPV-positive cervical cancer cells (HeLa, Caski, and clinical samples). Immunohistochemical data verified that immune reactivity for CD1d was completely abrogated in all cervical cancer lesions. Lack of CD1d expression in cancer-derived cells is unlikely to be associated with HPV E5 protein expression since the E5 gene is deleted when the HPV genome integrates into the host genome. Rather, CD1d may be genomically inactivated during carcinogenesis. Two of eighteen cases with CIN2 and CIN3 showed immune reactivity with the anti-CD1d MAb, although all lesions were positive for high-risk HPV. CD1d expression is known to be induced by inflammatory cytokines such as IFN-γ (9, 25). In some cases, an enhancement in CD1d expression secondary to the immunological microenvironment in the cervix *in vivo* may supercede E5-mediated downregulation. Alternatively, E5-mediated CD1d downregulation in CIN3 lesions may be lessened because most cells may have already integrated the HPV genome

and little E5 remains within the lesion. Statistical analysis, however, reveals a trend toward decreased CD1d expression with progressing CIN.

Previous investigations on HPV-associated immune evasion strategies have highlighted interference with adaptive immune responses against HPV through disruption of HLA molecules (19, 30). Here we focused on CD1d, which serves not only as a sentinel molecule in innate immune response but as a bridge between innate and adaptive immunity. Reports of CD1d expression in epithelial cells lagged behind its detection and functional studies in classic immune cells such as dendritic cells, macrophages, and B cells. In epithelial cells, CD1d encounters a wide array of pathogens and helps to orchestrate innate and adaptive immune responses to these immunologic challenges via interactions with CD1d-restricted iNKT. The interaction of CD1d with CD1d-restricted iNKT cell is lipid antigen dependent; however, this lipid antigen can be derived from invading microbes or from host cellular lipids. In response to some microbes, the rapid effects of CD1d-restricted NKT cells do not require recognition of microbial specific antigens (6, 34, 35). Since HPV has no envelope and therefore no HPV-specific lipid antigens, CD1d may present self lipid antigen for activation of iNKT cells in response to HPV-infected epithelial cells. Recognition of CD1d by iNKT cells can cause rapid release of both IL-4 and IFN-γ from the NKT cell (6). This would be predicted to activate CD1d-restricted iNKT cells and rapidly induce an adaptive immune response to invading microbes. Our previous investigations have also demonstrated that human reproductive tract epithelial cells that express CD1d on their cell surfaces are able to produce cytokines, including IL-12, in response to CD1d ligation (25). IL-12 is a central mediator in both innate and adaptive immunity and is crucial in the prevention of infectious diseases and tumors (40). IL-12 induces IFN-γ-producing NK, NKT, T helper, and cytotoxic T cells and thereby bridges innate and adaptive immune responses. Yue et al. have demonstrated that cross-linking of CD1d rapidly induces phosphorylation of IκB. This, in turn, promotes NF-κB activation and IL-12 production in monocytes and immature dendritic cells (43). As shown here, the induction of IL-12 production in response to CD1d cross-linking is completely abrogated in HPV E5-expressing epithelial cells but never to levels below those produced at baseline. The inhibition of CD1d-mediated cytokine production may be a mechanism by which HPV-infected cells evade (at least temporarily) the bridging of innate and adaptive immune responses that would otherwise occur upon interaction between cell surface CD1d and iNKT cells.

HPV E5 has been reported to play a role in HPV immunoevasion through the downregulation of cell surface HLA class I molecules. Several investigators have demonstrated that the papillomavirus E5 product inhibits the acidification of organelles, including the GA and endosomes (28, 32, 38). Ashrafi et al. have reported that the inhibition of GA acidification mediated by bovine papillomavirus E5 is associated with retention of MHC class I molecules in the GA (4, 41) and that HPV16 E5 retains HLA-A and -B, but not HLA-C and -E, within the GA. These authors hypothesize that the selectivity of HLA class I subtype downregulation may suggest that mechanisms other than GA acidification may be involved (2, 3). Gruener et al. demonstrated that interactions between HPV16 E5 and calnexin interfere with modification of HLA class I HCs and results in heavy-chain retention in the ER (21). Since the synthetic pathways for CD1d and HLA class I HCs are identical, we hypothesized that inhibition of calnexin folding capabilities by HPV E5 was a likely mechanism for decreased cell surface expression of CD1d in HPV-infected cells. Using confocal microscopy, we supported this hypothesis over the acidification mechanism by demonstrating that CD1d HC and calnexin colocalize in the ER rather than the GA. Interestingly, the CD1d HC that was rescued by MG132 treatment in E5-expressing cells was a 48-kDa mature form that was present in a diffuse pattern throughout the intracellular space (Fig. 8 and 9). It appears that CD1d synthesis and trafficking may be fairly robust in the presence of HPV E5 if proteasomal degradation is inhibited. This suggests that HPV E5 does not interfere with the synthesis of CD1d HC but rather delays its exit from the ER and alters its maturation so that CD1d HCs are targeted to proteasomal degradation. Interactions between HPV E5 and calnexin do not appear to interrupt all of the functions of calnexin, but just enough to co-opt the cellular cytosolic proteolytic pathway and effectively degrade CD1d and temporarily inhibits CD1d-mediated innate and adaptive immune pathways early in HPV infection.

CD1d expression and CD1d activation of neighboring iNKT cells may play an important role in the generation of innate and adaptive immune responses to microbial infection of the ectocervix. Our previous and current immunohistochemical data have shown that CD1d immunoreactivity and distribution patterns in ectocervix are similar to those in the penile urethra and vagina, where epithelial cells exhibit CD1d-mediated Th1-type cytokine production (25). It was likely that CD1d-bearing ectocervical epithelial cells were also capable of CD1d-mediated Th1-type cytokine production, and we have here shown that CD1d cross-linking on C33A/CD1d cells promotes the synthesis of IL-12. We therefore suggest a mechanism whereby CD1d downregulation in the presence of low- and high-risk HPV subtypes allows the infecting virus to evade host immune surveillance and establish persistent infection at the primary transmission site. The magnitude of HPV E5 expression and resultant CD1d downregulation may vary among CIN lesions, as shown in our clinical data. If so, variations in CD1d immunoreactivity in biopsy specimens of CIN lesions may be a predictive marker for the fate of early CIN. This topic is currently under investigation.

ACKNOWLEDGMENTS

This study was supported by a grant-in-aid from the Ministry of Health, Labor, and Welfare of Japan for the Third-Term Comprehensive 10-Year Strategy for Cancer Control; by a cancer research grant from the Ministry of Education, Culture, Sports, Science, and Technology of Japan; by a grant from Kanzawa Medical Research Foundation; and by a grant from the Okinawa New Industry Creation Project.

We are grateful to R. Blumberg (Harvard Medical School, Boston, MA), K. Oda (University of Tokyo, Tokyo, Japan), and D. J. Anderson (Boston University, Boston, MA) for kindly providing the CD1d-expressing retroviral plasmid pSRα-neo, the retrovirus expression system, and the vaginal epithelial cell line, respectively.

REFERENCES

1. **Araibi, E. H., B. Marchetti, G. H. Ashrafi, and M. S. Campo.** 2004. Downregulation of major histocompatibility complex class I in bovine papillomas. J. Gen. Virol. 85:2809–2814.